WORLD METEOROLOGICAL ORGANIZATION
GLOBAL ATMOSPHERE WATCH

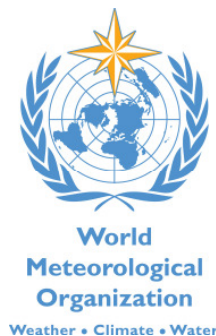No. 190

Instruments to Measure
Solar Ultraviolet Radiation

Part 3: Multi-channel filter instruments

Lead Author: G. Seckmeyer

Co-authors: A. Bais, G. Bernhard, M. Blumthaler, B. Johnsen, K. Lantz and R. McKenzie

Contributors: S. Diaz, P. Disterhoft, L. Jalkanen, A. Kazantzidis, P. Kiedron, B. Petkov, C. Sinclair and C. Wilson

World
Meteorological
Organization
Weather • Climate • Water

TABLE OF CONTENTS

1. INTRODUCTION

Ultraviolet radiation from the sun causes a considerable global disease burden including acute and chronic health effects on the skin, eye and immune system. Worldwide up to 60,000 deaths a year are estimated to be caused by ultraviolet radiation, most of which are due to malignant melanoma (Lucas et.al., 2008). Much of the UV-related illness and death can be avoided through a series of simple prevention measures. On the other hand, some UV is essential for the production of vitamin D in people. Emerging evidence suggests an association between vitamin D levels as an indicator of health risk [WHO, 2008] relating to some cancers, cardiovascular disease and multiple sclerosis among others, along with the established link with musculo-skeletal health.

This guide is part three of a series of documents dedicated to instruments for the measurement of solar ultraviolet radiation. These documents have been drawn up by the WMO Scientific Advisory Group on UV Monitoring and its UV Instrumentation Subgroup. The aim of the series is to define instrument specifications and guidelines for instrument characterization that are needed for reliable UV measurements. Part 1 of this series [Seckmeyer et al., 2001] describes scanning spectroradiometers that are able to separate the radiation in small wavelength bands with a typical resolution of 1 nm or less. Broadband instruments to measure erythemally-weighted ("sunburning") UV radiation are described in Part 2 [Seckmeyer et al., 2005]. The multi-channel filter radiometers (MCFRs) described here make measurements in several discrete wavelength bands with bandwidths of typically 1 to 10 nm fwhm (full width at half maximum). These instruments can be used to reconstruct spectra of solar global irradiance, to derive specific products such as erythemally weighted irradiance, or to determine total column ozone. Compared to spectroradiometers and broadband instruments, interpretation of data of these instruments is more complex and the separation of instrument characteristics and data products is not straightforward.

There is a diverse range of instruments that fall within this category. Their specifications must therefore be more flexible, while their detailed characterization becomes more important. At a minimum, the instruments must be capable of measuring global irradiances in at least two channels. The fore-optic generally consists of a diffuser, the angular response of which should ideally be proportional to the cosine of the zenith angle. The wavelength selection is typically achieved by narrow to moderate band interference filters, and the signal is detected with a photodiode or a phototube (without dynodes for multiplication). Data acquisition and logging are automated, and software is sometimes provided by the manufacturer to produce standardized products. Typically, the number of channels is larger than two, and some examples of these instruments include shadowbands which enable the near-simultaneous measurement of diffuse and direct irradiances, in addition to global irradiance.

Applications of such instruments are quite variable. For comparison with other instruments, the data processing usually requires some sort of normalization, convolution, or deconvolution. Examples of standard data products are discussed in Section 6.

The intended audience for this document includes scientists, instrument manufacturers, governmental organizations, and funding agencies dealing with UV monitoring and research. The document should serve as a guide and is based on the current experience and scientific knowledge about the measurement of UV radiation with multi-channel filter radiometers.

Advantages of multi-channel filter instruments

These instruments allow the determination of one or more of the following, normally by empirical or modelled relationships:

• Biologically effective doses for a variety of action spectra – without the requirement of supplementary ozone data.
• Total column ozone amount.
• Cloud attenuation, especially at high temporal resolution.
• Reconstruction of solar spectra at arbitrary wavelength resolution.

Compared to spectroradiometers (Part 1 of this series), they typically have a higher temporal resolution, a lower price, and are much simpler to operate. Compared to single-channel broadband instruments or broadband instruments measuring erythemally weighted solar radiation (Part 2 of this series) they allow separation of the influence of different atmospheric parameters affecting UV irradiance (e.g., total column ozone, cloud attenuation, aerosol effects, etc.). Furthermore, they are not restricted to only one action spectrum.

If equipped with a solar tracker or a shadowband they have the capability to determine direct solar spectral irradiance, both at the centre wavelength of the individual channels or at all wavelengths in the UV by means of spectral reconstruction. In this case, the Langley method may also be used as a calibration tool, to determine aerosol optical depths, or the extraterrestrial solar irradiance [Slusser et al., 2000].

Disadvantages of multi-channel filter instruments
- Compared to spectroradiometers, which deliver spectra, the signal output of multi-filter instruments usually requires post processing and the development of algorithms to gain meaningful results or measurement quantities.
- Although the stability of these instruments may match or exceed the stability of spectroradiometers, the absolute calibration is usually achieved by calibration against the latter. When calibrated against spectroradiometers, the uncertainty of multi-channel instruments is usually higher than that of spectroradiometers due to the additional transfer uncertainty.
- Multi-filter instruments can also be calibrated with Standards of Spectral Irradiance rather than by comparison with a spectroradiometer under the Sun. However, this calibration method requires laboratory characterization work, including the accurate characterization of the filter's response functions and angular response functions. This is particularly the case for channels in the UV-B, due to the great difference of lamp and the sun spectra. To obtain a small calibration uncertainty, accurate determination of the spectral responsivity is required. This in turn requires a tunable, small-bandwidth monochromatic light source of sufficient radiative power.
- Filters that are used for wavelength separation may be subject to drifts, both absolute and spectral, which are difficult to detect during operation.

2. OBJECTIVES

Multi-channel filter instruments can be employed for a variety of scientific applications. In a strict sense these instruments are capable of measuring only the global irradiance in the UV at several wavelength channels weighted with the response functions of the respective channel. However, the major advantage and present application for these instruments are the derived data products. In this respect these instruments differ from the other instruments described in the series (Part 1: Spectroradiometers; Part 2: Broadband Instruments Measuring Erythemal Irradiance; and Part 4: Array Spectroradiometers). The objectives for employing these instruments may be summarized as follows:

1. To derive data products such as erythemal irradiance with high temporal resolution.
2. To provide information on the variability of solar UV irradiance particularly due to clouds.
3. To contribute to determining geographic differences in UV and understanding their causes.
4. To derive spectral global irradiance in the UV at the instruments' nominal wavelengths. These data can be used to calculate spectral irradiance at other wavelengths.
5. To help in quality control (QC) of spectroradiometric UV measurements.
6. To support ground truthing of satellite estimates of UV.
7. To measure global 'response-weighted-irradiance' in the UV, which is the solar spectral irradiance weighted by the spectral response function of each channel.

As with spectroradiometers, multifilter-instruments may also be used to derive total column ozone and, in combination with a solar tracker or a shadowband, aerosol optical depth at various wavelengths.

3.   SPECIFICATIONS

Quantity	Quality
Cosine error	(a) < ±5% for incidence angles <60°
	(b) < ±5% to integrated isotropic radiance
	(c) < 3% azimuthal error at 60° incidence angle
Minimum spectral range	305-360 nm
Wavelength stability	< 0.03 nm for centre wavelength
Wavelength accuracy	Not applicable (see remark)
Bandwidth (fwhm)	< 10 nm
Bandwidth stability	< 0.04 * fwhm
Stray light including sensitivity to visible and IR radiation	< 1 % contribution to the signal of wavelengths outside 2.5 fwhm for SZA less than 70°
Stability in time on time scales up to a year	Signal change Currently in use: better than 5% Desired: 2%
Minimum number of channels	At least one channel with centre wavelength < 310 nm and at least one with centre wavelength > 330 nm
Maximum irradiance	Signal of the Instruments must not saturate at radiation levels encountered on the Earth's surface.
Detection threshold	SNR = 3 for irradiance at SZA=80° and total ozone column of 300 DU.
Instrument temperature	Monitored and sufficiently stable to maintain overall instrument stability
Response time	< 1 s
Multiplexing time	< 1 s
Accuracy of time	Better than ±10 s
Sampling frequency	$\leq$ 1 minute
Levelling	< 0.2°
Calibration uncertainty	< 10 % (unless limited by detection threshold)

Remarks on specifications:

• **Cosine error**
Smaller cosine errors would be desirable. Definitions of cosine and azimuthal error are given in the Glossary.

• **Minimum spectral range**
The minimum spectral range should be large enough to allow calculation of biologically effective irradiance (e.g., erythemal irradiance). Instrument channels should ideally cover the complete UV range as most biological systems respond to wavelengths in both the UV-B and UV-A regions.

• **Wavelength stability**
In principle, wavelength stability has to be within the given range for all observing conditions. This specification is hard to verify in the field, but can be approximately verified in laboratory experiments by characterizing the spectral response function as described in Section 5.1. . The specification of 0.03 nm was chosen, because calculations show that a shift of this magnitude leads to a change of up to 2% of the signal for a channel of 10 nm bandwidth centred at 305 nm for solar zenith angles between 0-80° degrees and ozone amount less than 500 DU. Calculations for smaller bandwidths do not change the conclusion appreciably. For more details see Annex C.1.

• **Wavelength accuracy**
This specification is not applicable for multifilter instruments because for meeting the objectives it is sufficient that the instrument's filter functions are characterized accurately. For further details see guidelines for instrument characterization in Section 5..

- **Bandwidth**

     The bandwidth of filters used in currently available instruments ranges between 1 and 10 nm. Instruments with small bandwidth typically require smaller corrections to convert their raw data to spectral irradiance (Section 4.1). For example, calculations presented in Annex C.3 show that transfer of calibrations from a lamp standard will result in an error of 200% in solar measurements at 305 nm for a bandwidth of 10 nm fwhm, SZA less than 80º, and total ozone between 250 and 450 DU, if no corrections are applied. The corresponding number for a bandwidth of 1.0 nm fwhm is 0.5 %. On the other hand a small bandwidth reduces the instrument's sensitivity, which makes it difficult to detect low-intensity radiation in the UV-B. The bandwidth is therefore a compromise between the competing requirements of being able to calibrate instruments accurately and to detect solar irradiance in the UV-B. Simulations provided in Annexes C.1 and C.2 show that accurate characterizations of the instrument channels' spectral response functions (including the accurate determination of the channel's centre wavelength) are more important than the bandwidth or the shape of response functions. These calculations indicate that data products such as total ozone and biologically effective irradiance can be calculated with similar accuracy from raw data of instruments with 1-nm or 10-nm wide channels.

- **Bandwidth stability**

     Calculations presented in Annex C.2 show that small changes in the bandwidth can have a significant effect on measurements of multi-filter instruments in the ozone cut-off region (wavelengths below 315 nm). For an instrument with a bandwidth of nominally 10 nm fwhm, a 0.2 nm broadening in bandwidth will result in up to 3% increase in the signal at 305 nm for SZA between 0° and 80°, and ozone amount between 250 and 450 DU. For narrower filters proportional changes in bandwidth are less of a concern.

- **Stray light, including sensitivity to visible and IR radiation**

     Multifilter instruments use interference filters to realize their spectral response functions. These filters may have secondary peaks in the visible and infrared, which may be outside the spectral range of the apparatus for measuring response functions. These secondary peaks can significantly contribute to the instrument's signal. This sensitivity should be checked with cut-off filters, (e.g., with WG or GG Schott longpass filters) using both Sun and calibration lamp as light source. A description of this technique can be found in Section 5.4.

- **Minimum number and wavelength of channels**

     By definition the instrument must have at least two channels. Normally these include one in the UV-B that is sensitive to total column ozone, and one in the UV-A. Depending on the application, e.g., deriving of biologically effective irradiance or aerosol parameters, additional channels are usually necessary. Centre wavelengths of existing instruments or other wavelengths relevant for specific applications can be found in Annex A.

- **Maximum irradiance**

     A compilation of the maximum UV irradiance to be expected at the Earth's surface is provided in Annex D.

- **Detection threshold**

     A low detection threshold is particularly necessary at locations where irradiance is low, e.g. at high-latitude sites or in winter.

- **Instrument temperature**

     Instrument temperature should be monitored and stabilized. Operating conditions logged should include the internal instrument temperature (specified by the manufacturer) and the effect of heating by solar radiation, which may warm the instrument by a considerable margin above the ambient temperature. Temperature stabilization is required for accurate measurements since both interference filters and photodiodes are temperature sensitive. If the correlation between temperature and sensitivity is well established the instrument may be used without stabilization by applying a temperature correction to the data. Temperature stabilization is preferable, since

temperature effects on filter-functions are difficult to correct.

- **Response time**

    A time constant of one second is sufficient for most applications and is easily achievable with the existing instrumentation. In some specialized applications, e.g., statistics for clear sky determination or the investigation of transient cloud effects, shorter time constants may be desirable.

- **Accuracy in time**

    Time errors of 10 s can lead to measurable differences as SZA and cloud conditions change. Time-keeping of better than 10 s is required if an instrument is to be compared to other instruments, in particular during cloudy situations. Uncertainties of less than one second are readily achievable with current technology (e.g., Internet time server, GPS).

- **Levelling**

    Levelling to better than ±0.2° can be achieved with a simple bubble level. Care should be taken that the reference plane used for levelling is parallel to the instrument's collector.

- **Sampling frequency**

    Less than 1 minute for most applications. However, for specific cloud studies, a much higher frequency (e.g., 1 s) may be necessary.

- **Calibration uncertainty**

    The calibration uncertainty includes all uncertainties associated with the irradiance calibration procedures.

Quality Assurance and Quality Control (QA/QC)

    To obtain data of high quality it is not sufficient that instruments meet the basic specifications discussed above. In addition, measurements of ancillary data for interpreting the measurements should be available, instruments have to be well maintained, and a Quality Assurance and Quality Control (QA/QC) plan has to be followed [Webb et al., 1998; 2003]. Recommended ancillary data and QA/QC procedures are compiled below.

- **Recommended ancillary data**
    - Total ozone column, from independent instruments or satellites to establish correction factors (Section 4) or to check for bias in ozone retrievals of multi-channel instrument data (Section 6.3).
    - Data from independent radiometers such as pyranometers, broadband UV sensors or spectroradiometers to help to validate the instrument's stability in time (Section 5.3).
    - Meteorological data.

- **Maintenance and QA/QC**
    1. Daily:
        - Checking of input optics (irradiance collector), and cleaning if necessary.
        - Determination of offset (Most instruments provide an automated offset-determination during the dark hours. Offset checks may have to be done manually in polar regions during periods with 24 hours of sunlight).

    2. Weekly:
        - Checking of the effectiveness of temperature stabilization, time-keeping, levelling, and data logging.

    3. At least once per year (every six months is desirable):
        - Checking of instrument's stability by comparison to a reference instrument, lamp, or spectroradiometer.
        - Checking of the correct operation and calibration of electronic supporting devices (data loggers, A/D boards, signal amplifiers, cables, computers etc.).

- Checking of dark stability during the year. Instability may suggest temperature dependence of the electronics or other problems.

4. At deployment and if quality checks above indicate a problem:
   - Verification of the spectral and angular response.
   - Checking of the accuracy of the instrument's level indicator. (The optical plane of an instrument is sometimes not consistent with the reference plane that is used for checking whether the instrument is level).

4.   CALIBRATION

There are several fundamentally different approaches to calibrating multi-channel filter instruments, some resulting in different radiometric quantities. Each approach can also be implemented in different ways. Several methods and their advantages and disadvantages are discussed below. Some implementations require that the spectral response functions of all channels are accurately known. Other methods are based on a comparison with a spectroradiometer under varying atmospheric conditions. In this case, measurements of spectral response functions may not be necessary. Approach 3 is applicable only to instruments equipped with shadowbands.

Approach 1 – Spectral Irradiance
The objective of Approach 1 is to establish a calibration **function** for each channel of the instrument which, when applied to the raw signal, returns <u>spectral irradiance at the nominal wavelength of the channel</u>. For example, a calibration function may be defined such that the calibrated measurement of each channel approximates spectral irradiance, measured by a spectroradiometer with a 1-nm bandpass at the channel's nominal wavelength. (This example assumes that spectroradiometer and filter instruments are exposed to the same radiation field.)

The advantage of Approach 1 is that the measurement — spectral irradiance — is a common radiometric quantity. The disadvantage is that calibration functions usually depend on the radiation source measured. This is particularly a problem for measurements in the UV-B part of the solar spectrum due to the rapid change of the Sun's spectrum with wavelength in this region. In this case, calibration functions will depend on solar zenith angle and other atmospheric parameters affecting the shape of the solar spectrum, such as total column ozone.

Approach 2 – Response-weighted irradiance
The objective of Approach 2 is to apply a calibration **factor** to each channel of the instrument such that the calibrated measurement of a given channel is response-weighted irradiance. This quantity is defined as the wavelength integral of the product of spectral irradiance and spectral response function of the channel (see Glossary). For example, if measurements from a spectroradiometer are weighted with the spectral response functions of a collocated filter instrument, the resulting response-weighted-irradiance will be identical with the calibrated measurement of the filter instrument.

The advantage of this calibration approach is that the calibration function simplifies to a factor, which is independent of the radiation source. When measuring solar radiation, this factor does not depend on solar zenith angle and other atmospheric parameters. If the calibration factor was established with a standard lamp, it can be applied to solar measurements without corrections. The disadvantage of the approach is that the quantity measured — response-weighted irradiance — is instrument dependent. Comparing the results of different instruments is therefore difficult. However, standardized data products such as erythemal irradiance can be calculated with good accuracy from calibrated values without the need of

considering the atmospheric conditions during the time of the measurement (Section 6.1).

Approach 3 – Langley Method
This approach is based on the Langley method and requires that instruments are equipped with shadowbands (Section 6.6). From consecutive measurements of global and diffuse irradiance (the latter determined by blocking the Sun with the shadowband), direct irradiance is calculated. Measurements of direct irradiance are performed at different airmasses and extrapolated to airmass zero to derive the instrument's signal that would be expected outside the Earth's atmosphere. The signals of the different channels at airmass zero are then compared with a reference extraterrestrial spectrum, which is weighted with the response function of each channel to establish calibration factors as in approach 2. These factors are finally applied to measurements of global irradiance. The method has been described by Slusser et al. [2000], and is not discussed in more detail here.

Implementations of Approach 1 and 2 are described in the following sections.

4.1 Calibration procedures based on Approach 1

4.1.1 Comparison with a spectroradiometer (spectral response functions NOT required)

For this method, the multi-channel instrument is operated next to a high-resolution spectroradiometer, both of which are exposed to sunlight. A calibration factor $C_i^{(1)}$ is established by dividing the net signal measured by channel i of the multi-channel radiometer, with spectral solar irradiance $E_S(\lambda_i)$, measured by the spectroradiometer at nominal wavelength λ_i:

$$C_i^{(1)} = \frac{V_{S,i}}{E_S(\lambda_i)} = \frac{(V_{S,i,G} - V_{S,i,0})}{E_S(\lambda_i)}.$$

Here $V_{S,i,G}$ is the "light" signal (e.g., measured in volts) of channel i when exposed to the radiation of the Sun, $V_{S,i,0}$ is the "dark" signal, obtained by covering the collector, and $V_{S,i}$ is the net signal, calculated as the difference of $V_{S,i,G}$ and $V_{S,i,0}$.

Measurements of the spectroradiometer have to be corrected for all systematic errors, such as the cosine error, prior to the comparison. Once $C_i^{(1)}$ has been derived, solar spectral irradiance at the nominal wavelength λ_i of the multi-channel radiometer is calculated with:

$$E_S(\lambda_i) = \frac{V_{S,i}}{C_i^{(1)}}$$

Due to the mismatch of the spectral response functions and the slit function of the spectroradiometer, $C_i^{(1)}$ will usually depend on solar zenith angle (SZA), total ozone (O_3), and other atmospheric parameters x. For this reason, $C_i^{(1)}$ is a function depending on these parameters:

$$C_i^{(1)} = C_i^{(1)}(SZA, O_3, x)$$

The argument (SZA, O_3, x) is omitted in the following for better readability.

The comparison of the multi-channel instrument and the spectroradiometer has to be performed over a period sufficient to include a large set of environmental conditions. Since the calibration function can be established only for conditions that occurred during the comparison period, deployment of the filter instrument at a location with different conditions may be problematic.

In practice, the dependence of $C_i^{(1)}$ on SZA, O_3, and other factors can be described with a lookup table or a numeric parameterization. For example, Díaz et al. [2005] used a multi-regressive model to parameterize the relationship between $V_{S,i}$, $E_S(\lambda_i)$, SZA and O_3:

$$\ln(E_S(\lambda_i)) = a_1 \ln(V_{S,i}) + a_2 O_3 + a_3 f(90^\circ - SZA) + b ,$$

where $f(90^\circ - SZA)$ is a function of SZA, and a_1, a_2, a_3, and b are coefficients determined by regression. Although parameterizations such as the one suggested by Díaz et al. [2005] may deliver sufficiently accurate results, great care must be applied when extrapolating parameterizations to conditions for which they were not designed. For example, a parameterization derived from measurements at a high-latitude location may lead to systematic errors if the instrument is deployed at a low-latitude site.

4.1.2 Comparison with a spectroradiometer (spectral response functions required)

As an alternative to the method described in Section 4.1.1, a calibration function may be established from a single "reference" solar spectrum that is measured by a multi-channel instrument and a spectroradiometer for well known SZA and atmospheric conditions. The alternative calibration function is denoted $C_i^{(2)}$ and includes a correction term $K_i^{(2)}$, which depends on SZA and O_3, and possibly other atmospheric parameters x.

$$C_i^{(2)} = \frac{V_{R,i}}{E_R(\lambda_i)} K_i^{(2)} = C_i^{(R)} K_i^{(2)} .$$

Here $E_R(\lambda_i)$ is solar spectral irradiance of the reference spectrum, $V_{R,i}$ is the net signal of channel i when measuring this spectrum, and $C_i^{(R)}$ is the calibration factor for the reference spectrum, calculated as ratio of $V_{R,i}$ and $E_R(\lambda_i)$. Solar spectral irradiance $E_S(\lambda_i)$ for arbitrary conditions is then calculated with:

$$E_S(\lambda_i) = \frac{V_{S,i}}{C_i^{(R)} K_i^{(2)}} = \frac{V_{S,i}}{C_i^{(2)}}$$

Note that this formula does not account for the cosine error of the instrument or any other systematic errors. In practice, it is usually necessary to correct for these errors (Section 5.5), leading to a further modification of the measurement equation:

$$E_S(\lambda_i) = \frac{V_{S,i}}{C_i^{(2)}} X_i(p_1, p_2, ..., p_n) ,$$

where $X_i(p_1, p_2, ..., p_n)$ is a correction term depending on n parameters such as SZA, O_3, and

cloud condition.

The correction function $K_i^{(2)}$ is defined by:

$$K_i^{(2)} = \frac{\int E_S(\lambda')R_i(\lambda')d\lambda'}{\int E_R(\lambda')R_i(\lambda')d\lambda'} \times \frac{E_R(\lambda_i)}{E_S(\lambda_i)}$$

where $R_i(\lambda)$ is the spectral response function of channel i. Systems for measuring the spectral response of filter radiometers are described in Section 5.1. Determination of $K_i^{(2)}$ requires the knowledge of the solar spectrum $E_S(\lambda_i)$, the quantity to be measured by the instrument. An exact determination of $K_i^{(2)}$ is therefore not possible. However, $K_i^{(2)}$ can be estimated from model calculation using SZA, O_3, and x as input parameters. For most applications knowledge of SZA and O_3 is sufficient. O_3 can be taken from satellite measurements. A compilation of radiative transfer models that can be used for the calculation of $K_i^{(2)}$ is provided in Annex B.

4.1.3 Transfer from standard of spectral irradiance

In this implementation, the radiometer is set up in front of a standard lamp. The spectral irradiance produced by the lamp at the place of the instrument's collector is denoted $E_L(\lambda_i)$; the associated net signal measured by channel i of the radiometer is $V_{L,i}$. The calibration factor $C_i^{(L)}$ is defined as the ratio of $V_{L,i}$ and spectral irradiance at the nominal wavelength λ_i of channel i:

$$C_i^{(L)} = \frac{V_{L,i}}{E_L(\lambda_i)}$$

With this definition, solar spectral irradiance at wavelength λ_i may be approximated with:

$$E_S(\lambda_i) \approx \frac{V_{S,i}}{C_i^{(L)}},$$

where $V_{S,i}$ is again the net signal of channel i when measuring the Sun.

Solar spectral irradiance calculated with this approach will have a large systematic error in the ozone cut-off region of the solar spectrum. The error increases with decreasing wavelength and increasing bandwidth of the radiometer's channel. It is caused by the difference of lamp and solar spectra at short wavelengths, where the second derivatives of both sources deviate considerably (Figure 1). For a hypothetical instrument with a centre wavelength of 305 nm, the error can be as large as 200% for an instrument with a bandwidth of 10-nm for SZA 0 – 80 and total ozone 250 – 450 DU. It is less than 1% for an instrument with a bandwidth of 1-nm.
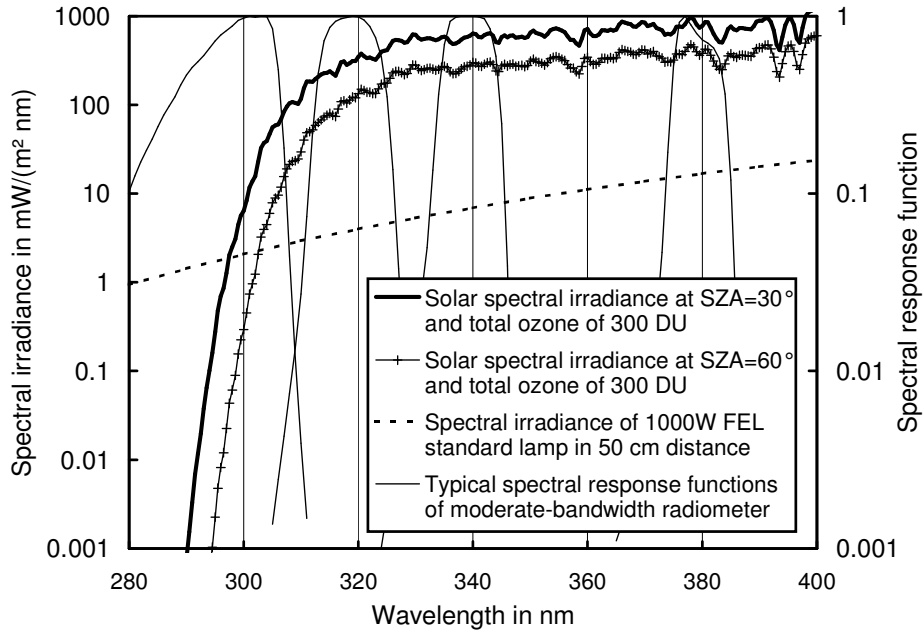
Figure 1 - Comparison of solar spectral irradiance at SZA=30° and 60°, the spectrum of a 1000-Watt FEL calibration standard at 50 cm distance, and typical response functions of a moderate-bandwidth multi-channel filter radiometer with nominal wavelengths of 305, 320, 340, and 380 nm and a bandwidth of approximately 10 nm.

To correct for the error, a correction function $K_i^{(3)}$ has to be applied for each channel, resulting in a modified calibration function $C_i^{(3)}$:

$$C_i^{(3)} = \frac{V_{L,i}}{E_L(\lambda_i)} K_i^{(3)} = C_i^{(L)} K_i^{(3)}$$

The correct expression for calculating solar spectral irradiance is then:

$$E_S(\lambda_i) = \frac{V_{S,i}}{C_i^{(L)} K_i^{(3)}} = \frac{V_{S,i}}{C_i^{(3)}}$$

Similar to the procedure described in Section 4.1.2, it is usually necessary to correct for additional systematic errors, such as the cosine error, leading to the following modification of the measurement equation:

$$E_S(\lambda_i) = \frac{V_{S,i}}{C_i^{(3)}} X_i(p_1, p_2,..., p_n),$$

where $X_i(p_1, p_2,..., p_n)$ is again a correction term depending on n parameters such as SZA, O_3, and cloud condition.

The correction function $K_i^{(3)}$ of channel i is defined as:

$$K_i^{(3)} = \frac{\int E_S(\lambda')R_i(\lambda')d\lambda'}{\int E_L(\lambda')R_i(\lambda')d\lambda'} \times \frac{E_L(\lambda_i)}{E_S(\lambda_i)}$$

Here $R_i(\lambda_i)$ is the spectral response of channel i. $K_i^{(3)}$ is a function of SZA, O_3, and other parameters affecting the transfer or radiation through the atmosphere, and can be estimated from modelled spectra in a similar manner as $K_i^{(2)}$. For most applications, knowledge of SZA and O_3 is sufficient.

For lamp-based calibrations, $R_i(\lambda_i)$ must be known very accurately. According to Annex C.1, the wavelength applicable to a given spectral responsivity needs to be known to an accuracy of 0.03 nm to give an error in the solar irradiance of less than 2% for a filter with centre wavelength at 305 nm. The error in the signal is essentially independent of the fwhm of the radiometer for bandwidths from 1 – 10 nm and the error is smaller with increasing centre wavelength.

4.1.4 Empirical calibration approaches

The dependence of the calibration function on SZA and O_3 can partly be accounted for by including measurements of all channels in the calibration [Díaz et al., 2005]. For example, solar spectral irradiance at wavelength λ_i may be expressed as a linear combination of net signals measured by all channels:

$$E_S(\lambda_i) = \sum_j c_{ij} \, V_{S,j}$$

The coefficients c_{ij} are determined via multi-linear regression of solar spectral irradiance $E_S(\lambda_i)$, measured with a spectroradiometer under varying conditions, against net signals $V_{S,j}$, measured with the multi-channel radiometer at channels j. To further minimize errors caused by the SZA-dependence of the calibration, Díaz et al. [2005] suggested the following modifications to the regression equation:

For SZA < 40°:
$$E_S(\lambda_i) = [\sum_j c_{ij} \, V_{S,j}] + c \times f(90^\circ - SZA)$$

For SZA > 40°:
$$\ln(E_S(\lambda_i)) = [\sum_j c_{ij} \, \ln(V_{S,j})] + c \times f(90^\circ - SZA) + d$$

where $f(90^\circ - SZA)$ is a polynomial fit-function, and c and d are fit-coefficients.
Empirical approaches should be validated over a large range of conditions with differing SZA, O_3, and other parameters x, and should not be applied to conditions outside this range.

4.1.5 Comparison with a reference instrument

In this case, the instrument to be calibrated should operate alongside a reference multi-channel instrument ("R") with well-established calibration factors $c_i^{(R)}$, which are generally dependent on SZA and O_3. If the spectral response functions of the two instruments are virtually identical for all channels, the calibration factor $c_i^{(T)}$ of the instrument under test ("T") is:

$$c_i^{(T)} = \frac{V_i^{(T)}}{V_i^{(R)}} \times c_i^{(R)}$$

By this comparison, also $c_i^{(T)}$ will also become dependent on SZA and O_3. The instruments should run side-by-side for several days covering a full range of SZA, and ideally a wide range of ozone columns. If the spectral response functions of the two instruments are different, a correction

11

factor must be applied, which can be calculated in a similar way as described in Section 4.1.2.

4.2 Calibration procedures based on Approach 2

In this approach, the calibration factor C_i^* is the ratio of the net signal of channel i, V_i, to irradiance $E(\lambda)$, weighted with the relative spectral response $R_i(\lambda)$ of channel i:

$$C_i^* = \frac{V_i}{\int E(\lambda) R_i(\lambda) d\lambda}$$

The radiation source producing $E(\lambda)$ can either be a standard lamp or the Sun. In the former case, $E(\lambda)$ is known from the standard's certificate; in the latter case, $E(\lambda)$ is typically measured by a spectroradiometer deployed next to the filter instrument to be calibrated. In theory, C_i^* does not depend on the light source being measured, which can be the Sun or any artificial light source. In practice, C_i^* is subject to uncertainty if $R_i(\lambda)$ is not accurately known. The uncertainty of C_i^* as a function of various characteristics of $R_i(\lambda)$ are discussed in Annex C. The radiative quantity being measured by filter instruments calibrated with this approach is "response-weighted irradiance" E_i with

$$E_i = \frac{V_i}{C_i^*}$$

This quantity is different for every instrument. However, standardized data products such as erythemal irradiance can be calculated from E_i with high accuracy. This is discussed in Section 6.

5.   CHARACTERIZATION OF MULTI-CHANNEL FILTER INSTRUMENTS

Proper characterizations of angular and spectral response of multi-channel filter instruments are crucial for obtaining accurate measurements. Information from the characterization is used to convert raw signals of the instruments to physical quantities such as spectral irradiance. For appropriate quality control and assurance of filter instruments, characterization of the spectral response and angular response should be undertaken at regular intervals. Characterizing instruments requires well-designed systems. It is suggested that qualified laboratories carry out spectral response and cosine response characterizations. In addition, the stability and calibration of any instrument needs to be monitored over time. The following gives a general description of typical characterization systems and procedures.

5.1   Characterization of spectral response functions

The spectral sensitivity of each channel should be measured with a dynamic range and wavelength range large enough to detect small filter leakages outside the main filter bandpass. Generic response functions should not be used because it has been shown that the spectral transmission of filters may vary significantly, even for filters of the same batch [Bernhard et.al., 2005]. The centre (nominal) wavelength of each channel should be calculated from the measurement response functions, e.g. (1) Determine centroid wavelength of the response function, (2) Multiply the response function with a reference spectrum and determine its centroid wavelength.

A system for characterizing the spectral response of multi-channel radiometers requires a spectral light source. This can be provided either by a tunable laser or by an optically dispersing instrument, such as a monochromator. The following description will concentrate on the latter. Typically, the output from a high-intensity light source such as a xenon arc lamp is imaged onto the

entrance slit of a monochromator. The monochromator scans across the desired wavelength range (e.g., 270 – 420 nm) in wavelength increments small enough to resolve the spectral response. The output of the monochromator is imaged onto one of two separate detection systems, the multi-channel filter radiometer (MCFR) under test and a reference detector with known spectral response. A measurement of the MCFR and the reference detector output signals are taken at each wavelength step. The spectral response $R_i(\lambda_i)$ of the MCFR is calculated from measurements of the MCFR and the reference detector:

$$R_i(\lambda_i) = \frac{(V_{DUT,i,L}(\lambda_i) - V_{DUT,i,0}(\lambda_i))}{(V_{R,L}(\lambda_i) - V_{R,0}(\lambda_i))} S_R(\lambda_i)$$

Here $V_{DUT,i,L}(\lambda_i)$ is the "light" signal of channel i of the MCFR, $V_{DUT,i,0}(\lambda_i)$ is the corresponding dark signal, $V_{R,L}(\lambda_i)$ and $V_{R,0}(\lambda_i)$ are the light and dark signal of the reference detector, respectively, and $S_R(\lambda_i)$ is the spectral response of the reference detector. Instrument specific spectral response functions may be available from the manufacturer, but can change with time. The reference detector SRF should ideally be confirmed by a standards laboratory, and must be checked periodically to assure stability. Measuring $R_i(\lambda_i)$ accurately in absolute terms is difficult and it is therefore conventional to normalize $R_i(\lambda_i)$ to one at its maximum value.

The monochromator's bandwidth should ideally be more than an order of magnitude smaller than the bandwidth of the MCFR. Its wavelength accuracy should be better than 0.03 nm for filters centred at 305 nm to achieve solar irradiance errors less than 2% (see Annex C.1), in particular if the MCFR is calibrated against a lamp (Section 4.1.3) This criterion is less strict when measuring spectral response at longer wavelengths. The stray-light rejection of the monochromator should be sufficient to ensure spectral purity at each measurement step. This typically requires the use of a double-monochromator. The light output from the monochromator should be sufficient to give a dynamic range of at least three orders of magnitude in the measured spectral response of the MCFR. The spectral response measurement system should have an optimum balance between acceptable stray-light rejection, band-pass size, wavelength step size and adequate signal throughput to obtain the spectral response curve of the MCFR with the desired dynamic range.

It is often not possible to set the monochromator to a bandwidth that is one order of magnitude smaller than that of the MCFR's channels, and still have sufficient signal over the desired dynamic range. It may therefore be necessary to deconvolve the spectral response function with the monochromator's slit function. A suitable technique has been suggested by Bernhard et al. [2005]. As an alternative, the "core" part of the response functions may be scanned with a small bandwidth and the "wings" with a large bandwidth to have sufficient signal. Measurements with the two bandwidth settings can then be "stitched" together. This technique has been successfully used by Johnsen et al. [2008b].

Spectral response functions should ideally be characterized once per year. This is often not possible in practice. At a minimum, instruments should be retested if comparisons with other instruments indicate potential changes in the detector's spectral response.

The following publications provide descriptions of systems for the characterization of spectral response functions: Bernhard et al. [2005]; Bolsée et al. [2000]; di Sarra et al. [2002]; Hülsen and Gröbner [2007]; Johnsen et al. [2008b]; and Lantz et al. [2005]. These papers should be consulted if a user of multi-channel instruments chooses to perform such characterizations himself. As these measurements are rather demanding, it is advised these characterizations are performed by established laboratories such as the WMO/GAW regional calibration centers.

5.2   Angular response

As with any other instrument measuring solar UV irradiance the angular response of a multi-channel filter instrument should be characterized for zenith angles between -90° and 90°, and several azimuth angles in increments sufficient to obtain any structure that may be present (e.g., 1° zenith angle increment, 45° azimuth angle increment).

The system for measuring the angular response typically consists of a light source, a computer-controlled rotary table, and alignment fixtures. The MCFR is mounted to the rotary table such that its axis of rotation "touches" the reference plane of the MCFR's diffuser. For performing the angular response measurement, the rotary table is turned from -90° to 90° while the signals of the MCFR detectors are recorded. The measurement is repeated after turning the instrument in its holder to a different azimuth angle. Cosine and azimuthal errors can be calculated from these measurements using the definitions given in the Glossary.

The light source may either be a high-intensity incandescent lamp, such as a 1000-W FEL lamp, or a discharge lamp, such as a Xenon lamp. If a convex mirror or a lens is used to collimate the lamp's output, it has to be ensured that the beam is homogeneous and overfills the diffuser of the MCFR.

The measurement system should have optically flat black surroundings to limit scattered light. A large baffle should be installed between lamp and MCFR such that scattered off-axis radiation from the lamp cannot reach the MCFR.

For accurate measurements it is critical that the MCFR is aligned correctly. This can be achieved by means of an alignment laser mounted behind the light source and directed toward the rotary stage. First, lamp and MCFR are aligned such that the laser goes through the centre of the lamp and the centre of MCFR's diffuser. Second, a mirror is placed in front of the MCFR such that it is parallel to the MCFR's reference surface used for levelling the instrument in the field. The alignment of the MCFR is then adjusted such that the laser beam is back-reflected to the laser. With this method the 0° position of the rotary stage can also be determined accurately.

If the measurements indicate that the instrument has a significant azimuthal error, it is important that the orientation of the instrument can be marked and transferred to the field such that azimuthal asymmetries in solar measurements can be interpreted and corrected.

The following publications provide descriptions of systems for the angular response characterizations: Harrison et al. [1994a]; Hülsen and Gröbner [2007]; Johnsen et al. [2008b].

5.3   Stability tests

Several methods can be used to check the temporal stability of the calibration of multi-filter instruments. These include:

- Comparison with solar measurements performed by well-maintained spectroradiometers.
- Comparison with other multi-filter instruments .
- Via the Langley Method of analysis and extrapolation to extraterrestrial solar irradiance.
- A combination of the methods listed above.

5.3.1   Comparison with spectroradiometers

For the implementation of this method, the multi-filter radiometer to be tested and the spectroradiometer measure side by side for a period of ideally one week or longer. The measurements of the spectroradiometer are weighted with the response functions of the multi-filter radiometer as described in Section 4.2, and compare with the net signal of the multi-filter radiometer. The ratio of the two measurements should ideally not depend on time. If the drift is beyond an acceptable limit, the multi-filter radiometer should be recalibrated. The method is routinely applied to measurements performed by the NSF UV Monitoring Network [Bernhard et al., 2008].

5.3.2 Comparison with a reference multi-filter radiometer

As in the previous section, the multi-filter radiometer to be tested and the reference radiometer measure side by side for a sufficiently long period. Measurements of the two instruments are compared as described in Section 4.1.5. Both instruments should ideally have very similar spectral response functions. If this is not the case, the time series analysis should be restricted to a subset of measurements performed at similar SZA and total ozone column.

5.3.3 Calibrations with standards of spectral irradiance

The multi-filter radiometer to be tested is regularly (e.g., annually) placed in front of a Standard of Spectral Irradiance and the net-signal is measured. Assuming that the lamp is stable, the radiometer should measure the same net-signal at every event. If different lamps are used, measurements of the radiometer should be converted to spectral irradiance and compared with the values provided in the lamp's certificates. Additional corrections similar to those described in Section 4.1.3 may be necessary if the colour temperature of the various lamps is not identical. Calibration standards, either reference standards or working standards, should be recalibrated (or replaced) after 20 hours of use, unless otherwise stated in the lamp's certificate. A recalibration of reference standards should be performed by standard laboratories (see also Webb et.al., 1998)

5.3.4 Repeated spectral response measurements

Repeated spectral response measurements can help to determine reasons for changes in instrument sensitivity uncovered by one of the three methods described above. For example, these measurements may detect changes in the response functions' centre wavelengths, bandwidth, peak response, and "wings" [Bigelow and Slusser, 2000]. Figure 2 presents a time series of centroid wavelengths and bandwidths determined from measurements of an instrument that is used by the USDA UV-B Monitoring and Research Programme.
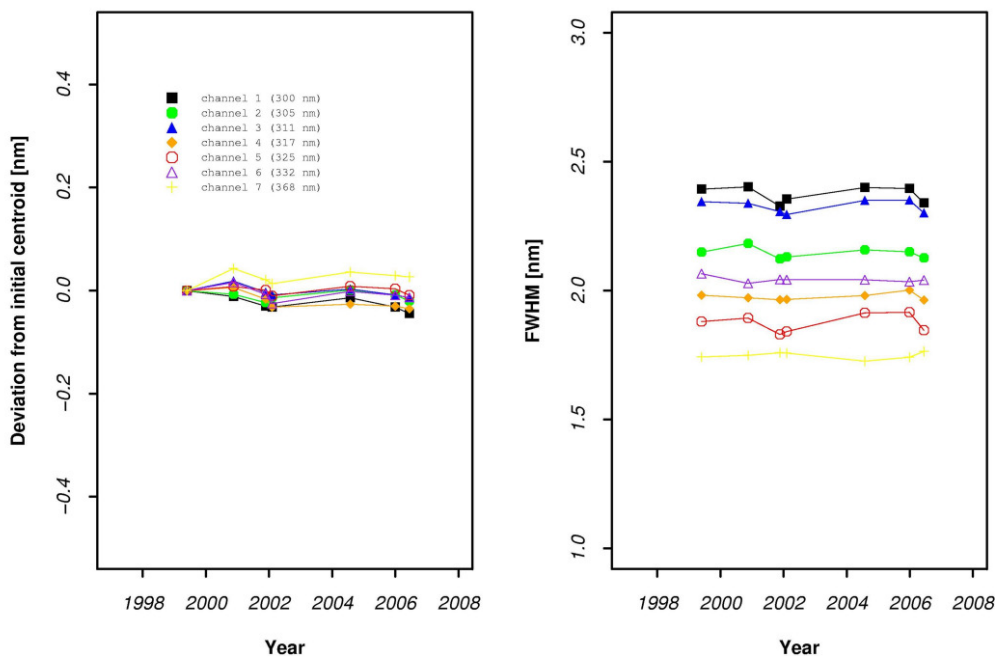
Figure 2 - Results of repeated spectral response measurements of a instrument used by the USDA UV-B Monitoring and Research Programme. Left panel: deviation of centroid wavelength from initial measurement. Right panel: Bandwidth expressed as fwhm.

5.3.5 Langley Method

The Langley method allows determination of the solar spectrum outside the Earth's atmosphere from measurements at various airmasses [Slusser et al., 2000]. Application of the technique is possible only for instruments that are equipped with a shadowband. If the radiometer is stable, repeated estimates of the extraterrestrial spectrum should ideally be identical. The technique is mostly suited to detect long-term changes of an instrument's stability as the Sun is a very stable light source. The method is not affected by changes in reference instruments or lamps

that might affect the methods described in Sections 5.3.1 - 5.3.3. However, the Langley method gives robust results only if the atmosphere is stable during the Langley analysis, for example this requires that the sky is cloud-free and atmospheric ozone and aerosol concentration are constant over the time required for a Langley analysis (typically a few hours are needed). Apart from high altitude sites, these conditions are rarely met. More information on the Langley method is provided in Section 6.6.

Bigelow and Slusser [2000] have compared the methods described in Sections 5.3.3, 5.3.4, and 5.3.5 and discussed their advantages and disadvantages. More information on long-term stability of multi-channel instruments can also be found in Johnsen et al. [2002], Janson and Slusser [2003], and Janson et al. [2004].

5.4   Visible and infrared leakage test
The sensitivity to visible and infrared radiation can be tested with cut-off filters that transmit visible and infrared radiation but block UV radiation (e.g., GG 400 produced by Schott). The measurement should be performed outdoors with the Sun as the light source. The filter should be placed on top of the radiometer's diffuser. It is important that there is a good light-tight seal between filter and radiometer to prevent unfiltered radiation from reaching the diffuser. With the filter in place the signal should be less than 1% compared to the signal without the filter for SZA smaller than 70°. If the instrument is calibrated with a Standard of Spectral Irradiance (Section 4.1.3), then the light leakage should also be tested using the same calibration lamp. This is important as incandescent lamps have a larger contribution from the infrared than the Sun [Lantz et al., 2005].

5.5   Cosine error correction
The effect of the cosine error on solar data should be corrected. Correction methods must take into consideration: (1) the deviation of the directional response of the radiometer from the ideal cosine response and (2) the distribution of the radiation field, i.e., the distribution of radiance, when measuring solar radiation. Because the radiation field is generally not known in detail, approximations have to be made. The most common approximations and simplifications are:

- The global spectral irradiance is defined as the sum of direct horizontal spectral irradiance and diffuse spectral irradiance. For clear-sky conditions, the proportion of both can be either measured directly or calculated by a model. For overcast conditions, the direct spectral irradiance is set to zero. For partly cloudy conditions, the accuracy of cosine error correction methods is generally limited.
- The directional distribution of sky radiance is regarded as isotropic. This assumption has proved to be approximately valid in the UV-B region (Blumthaler et al., 1996).

Methods of cosine error corrections should provide estimates of their uncertainty. Description of implementations and validations of cosine error correction algorithms can be found in (Bernhard and Seckmeyer, 1997), (Seckmeyer and Bernhard, 1993), (Gröbner et al., 1996), (McKenzie et al., 1992), (Feister et al., 1997), (Bais et al., 1998) and (Cordero et.al.,2008).

6.   APPLICATIONS

Several data products can be derived from multi-channel filter instruments including biologically effective irradiance (such as erythemal irradiance), reconstructed high-resolution solar spectra, total column ozone, and aerosol and cloud optical depth. The following section gives an overview of methods for calculating these data products.

6.1   Biologically effective irradiance
The following methods are suitable for deriving values of biologically weighted irradiance (such as erythemally weighted irradiance) from measurements of multi-channel filter instruments.

6.1.1 Calculation of biologically effective irradiance via regression analysis

Biologically effective irradiance *D* (see Glossary) is estimated via the linear equation

$$D = \sum a_i V_i ,$$

where V_i are the net signals of the instrument's channels. The coefficients a_i are determined via multiple linear regression against *D* determined from high-resolution spectra measured with a collocated spectroradiometer. For most accurate results all systematic errors of the spectroradiometer, such as the cosine error, have to be corrected.

Results obtained with this regression method are usually affected by systematic errors, which depend on SZA and total ozone O_3. Results can be improved by multiplying the results of the regression, D_{regress}, with a correction function $\varepsilon(SZA, O_3)$. In practice, it is sufficient to consider the effect of the SZA only. In this case, the correction function simplifies to $\varepsilon(SZA)$:

$$D_{\mathrm{corrected}} = \varepsilon(SZA) \cdot \sum a_i V_i = \varepsilon(SZA) \cdot D_{\mathrm{regress}}$$

The function is determined with a two-step process: first, *D* obtained from the spectroradiometric measurements is ratioed against D_{regress} and plotted versus SZA. In a second step, $\varepsilon(SZA)$ is determined by fitting a polynomial to the data of this scatter plot. The method has been described in detail by Johnsen et al. [2008a; 2008b].

6.1.2 Method suggested by Dahlback [1996]

This method is based on calibration Approach 2 (Section 4.2) and requires a set of linear equations to be solved. The solution of the set of equations gives coefficients a_i, which allow the calculation of biologically effective irradiance *D* via $D = \sum\limits_{i} a_i V_i$, similar to the method described in Section 6.1.1.

Method in detail:

- The net signal V_i of channel i is:

$$V_i = \int_0^\infty C_i^* R_i(\lambda) E(\lambda) d\lambda \approx \sum_{\lambda=0}^{\infty} C_i^* R_{i\lambda} E_\lambda \Delta\lambda$$

This equation follows immediately from the definition of C_i^* introduced in Section 4.2. C_i^* can be derived from one single solar spectrum measured with a high-resolution spectroradiometer next to the multi-channel instrument.

- The exact biologically effective irradiance D_{exact} is defined by (see Glossary):

$$D_{\mathrm{exact}} = \int_0^\infty W(\lambda) E(\lambda) d\lambda \approx \sum_{\lambda=0}^{\infty} W_\lambda E_\lambda \Delta\lambda ,$$

where $W(\lambda)$ is the biological weighting function.

- D_{exact} can be approximated by $D_{approx} = \sum\limits_{i=1}^{m} a_i V_i$, where *m* is the number of channels of the multi-channel instrument.

- By setting $D_{\text{approx}} = D_{\text{exact}}$ and replacing V_i by the first equation leads to

$$\sum_{i=1}^{m}\left(a_i C_i^* \sum_{\lambda=0}^{\infty} R_{i\lambda} E_\lambda\right) = \sum_{\lambda=0}^{\infty} W_\lambda E_\lambda$$

   This set of m equations can be solved with *m* different solar spectra, modelled for different SZA and total column ozone. *Dahlback* [1996] uses 4 spectra with SZA of 40° and 60° and total ozone columns of 320 and 340 DU.

- The accuracy of the dose-rate estimate D_{approx} thus derived depends slightly on SZA and total ozone column, requiring a correction term $\varepsilon(SZA, O_3)$, similar to the method described in Section 6.1.1. With this correction applied, the accuracy of the method for 0° < SZA < 80°, cloud optical depth between 0 and 60, and ozone between 200 and 500 DU, is estimated to be better than 5% for the instrument chosen by *Dahlback* [1996].

   The method suggested by Dahlback has been implemented by the Norwegian UV-monitoring programme [Johnsen et al., 2002] and the U.S. National Science Foundations UV Monitoring Network for Polar Regions [Bernhard et al., 2005]. In the latter reference, data products for more than 15 different action spectra are introduced, in addition to erythemally weighted irradiance.

6.1.3 Calculation of biologically effective irradiance from reconstructed spectra
Biologically effective irradiance *D* can be directly derived from reconstructed spectra (Section 6.2).

$$D = \int_0^{\infty} W(\lambda) E_{\text{reconstructed}}(\lambda) d\lambda$$

6.2 Calculation of high-resolution spectra
Solar high-resolution (e.g., 1-nm) spectra may be calculated from multi-channel filter radiometer data based on the following methods. The major characteristics of these methods are listed below. For a detailed analysis, please refer to the original papers.

6.2.1 Method suggested by Dahlback [1996] and Booth [1997]
In a first step, total column ozone and cloud optical depth are determined as described in Sections 6.3. and 6.4. Information on albedo and aerosol optical depth is obtained from measurements of other instruments or from a climatology. In a second step, a high-resolution solar spectrum is calculated with a radiative transfer model and the previously derived input parameters. References to suitable radiative transfer models are given in Annex B.

6.2.2 Method suggested by Min and Harrison [1998]
For this method, the spectrum to be determined is written as a product of extraterrestrial spectrum and atmospheric transmission. The atmospheric transmission is constructed as an analytical function with several coefficients X_j. In the second step, these coefficients are determined by non-linear least-square fit calculation, resulting in the spectrum sought.

Method in detail:

The least square-fit is based on minimizing the sum

$$\frac{1}{m}\sum_{i=1}^{m}(E_i - F_i)^2$$

where E_i is the measured irradiance of channel i of the multi-filter instrument (1<= i <= Total number of filters) and F_i is the integral

$$F_i = \int_0^\infty R_i(\lambda) \times \text{synthetic\_spectrum}(\lambda, \mathbf{X}) d\lambda = \int_0^\infty R_i(\lambda) S(\lambda) T(\lambda, \mathbf{X}) d\lambda$$

In this equation, $R_i(\lambda)$ is the spectral responsivity of the filter i. The synthetic spectrum is constructed as the product of an extraterrestrial spectrum $S(\lambda)$ and an atmospheric transmission function $T(\lambda, X)$, which depends on a set of parameters **X**. (See Min and Harrison [1998] for derivation of the function $T(\lambda, X)$.)

Before the least squares fit can be carried out, the multi-channel instrument has to be calibrated based on Approach 2 (Section 4.2).

A comparison of synthetic spectra retrieved with this method with spectra measured by spectroradiometers has been presented by Gao et al. [2002]. The accuracy of the method has been further improved by Davis and Slusser [2005].

6.2.3   Method suggested by Fuenzalida [1998]
This method is based on a constrained inversion algorithm. See paper for details.

6.2.4   Method suggested by Thorseth and Kjeldstad [1999], and Thorseth et al., [2000]
The method utilizes both a scanning spectroradiometer and a multi-channel radiometer. The spectroradiometer provides high spectral resolution while the multi-channel radiometer gives high temporal resolution. Combining both systems provides solar spectra in high temporal resolution (e.g., 0.5 Hz), which may be useful for studying cloud effects.

Advantages of the method
- No radiative transfer modelling required; error sources such as unknown model input-parameters (e.g., albedo, aerosols, and broken-cloud effects) are inherently excluded.
- High temporal resolution.
- No absolute calibration of the multi-filter instrument is required. The only requirements are a good short-term stability (stable to within 10 minutes), good linearity and spectral response at a well defined wavelength. The overall accuracy is mainly based on the calibration and the characteristics of the spectroradiometer.

Disadvantage of the method
- Additional spectroradiometer required.

See paper by Thorseth and Kjeldstad [1999] for implementation of method.

6.2.5   Spectral reconstruction with neural networks algorithm
A method for reconstructing high-resolution spectra from measurements of multi-filter radiometers based on a neural networks algorithm has been suggested by Feister et al. [2005]. Additional details of the algorithm are provided by Schwander et al., [2001].

6.3   Calculation of total column ozone

6.3.1   Method suggested by Dahlback [1996]
This method is based on a modified algorithm suggested by Stamnes et al. [1991], which was developed for deriving total column ozone from global irradiance spectra. The implementation suggested by Dahlback [1996] is based on the following equation:

$$V_i / V_j = \left(\sum_{\lambda=0}^{\infty} C_i^* R_{i\lambda} E_\lambda \right) \Big/ \left(\sum_{\lambda=0}^{\infty} C_j^* R_{j\lambda} E_\lambda \right) \equiv N$$

The right side of this equation is calculated with a radiative transfer model for a wide range of SZAs and total column ozone O_3 using spectral response functions ($R_{i\lambda}$ and $R_{j\lambda}$) of two channels (i and j) of the filter radiometer. The nominal wavelength of one channel must be in a spectral region that is sensitive to ozone absorption, the other channel must be at a wavelength that is less affected by ozone absorption. A look-up table is constructed from these calculations, specifying N in dependence of SZA and O_3. In a second step, the ratios of the measured signals of channel i and j, V_i and V_j, are compared with the N-ratios in the look-up table given at the SZA of the measurement, resulting in an estimate for O_3. Both Dahlback [1996] and Stamnes et al. [1991] base the calculation on the wavelength pair 305 nm (sensitive to ozone) and 340 nm (insensitive to ozone). The accuracy was determined by comparison with Dobson and Brewer measurements. Deviations were found to be smaller than a few percent.

6.3.2   Method suggested by Slusser [1999]

This method is similar the approach by Dahlback [1996], and is also based on a modified "Stamnes"-method. The wavelength pair is 300 (sensitive to ozone) and 338 nm (insensitive to ozone). The paper gives detailed information on influence of atmospheric and other parameters on the accuracy of the ozone estimate. These include: atmospheric pressure, aerosols, cloud cover, asymmetry factor, single-scattering albedo, ground albedo, ozone absorption coefficients used by the model, atmospheric temperature profiles, change in spectral response of filters, signal-to-noise ratio, and cosine-error.

6.4   Calculations of cloud optical depth [Dahlback, 1996]

Response-weighted irradiance for a radiometer channel in the UV-A is calculated with a radiative transfer model for different cloud optical depths, and a look-up table is created. In a second step, solar measurements of this channel are compared with the values in the look-up table to derive cloud optical depth. As one-dimensional radiative models can describe only stratiform clouds, the application of the method is problematic for general cloud conditions.

6.5   Quality control of spectroradiometers

Spectroradiometers can be more prone to short-term instabilities than multi-channel filter instruments due to their more complex design. Comparisons of measurements from spectroradiometers and multi-channel instruments on an operational basis can help to uncover problems, track the stability of the spectroradiometer and initiate remedial action. For a most efficient comparison, the net signals V_i of the multi-channel instrument should be compared with response-weighted irradiance calculated from spectroradiometric measurements. An application example is provided by Bernhard et al. [2008].

6.6   Langley Method

The Langley Method is based on the work of S. P. Langley in the early 1900s to determine the solar constant. If the instrument is equipped with a movable shadowband or if it is mounted on a solar tracker and equipped with a field-of-view limiting baffled tube, direct measurements of solar irradiance can be performed. When a shadowband is used, direct irradiance is derived by subtracting diffuse irradiance with the shadowband in place from global irradiance measurements with the shadowband removed from the light path. Based on direct measurements and the airmass, so-called Langley plots can be performed [Slusser et al., 2000]. This technique allows several evaluations:

- By extrapolation of the direct measurements at different solar zenith angles (or different airmasses) spectral irradiance at the top of the atmosphere (i.e., the extraterrestrial solar spectrum) can be derived. These measurements can be compared to an extraterrestrial solar spectrum from the literature to regularly check the calibration

coefficients of the multi-filter instrument. With this technique it is possible to use the Sun as the calibration source for UV measurements.

- From measurements at different wavelengths, values of total column ozone, aerosol optical depth (including wavelength dependence of aerosol parameters) can be derived. With sophisticated analysis algorithms and if measurements at appropriate wavelengths exist, aerosol size distributions, and columnar amounts of water vapour and nitrogen dioxide may also be extracted.

A Langley plot is possible only if the atmosphere is stable for a sufficient amount of time, i.e. the optical depths of Rayleigh and aerosol scattering as well as ozone absorption should be constant over a range of at least 3 airmasses. Best conditions for Langley plots are usually found on mountains with altitudes of 2500 meters or higher. Varying conditions near cities may only sporadically be suitable.

Good introductions to the Langley Method using filter instruments can be found in the works by Schmid and Wehrli [1995]; Schmid et al. [1998]; Harrison and Michalsky [1994a]; Harrison and Michalsky [1994b]; and Slusser et al., [2000]. Note that these literature examples are not a complete list of all the valuable work that has been done concerning the Langley Method.

———————

GLOSSARY

Action spectrum
See biological weighting function.

Airmass
Airmass (or more precisely "relative optical airmass") is defined as the ratio of the actual (slant) optical path length taken by the direct solar beam to the analogous vertical path when the Sun is overhead from the surface to the top of the atmosphere.

Azimuthal Error
The azimuthal error f_a describes the variation of the angular response of a radiometer at a fixed incidence angle ε as a function of the azimuthal angle φ. It is defined by

$$f_a(\varepsilon,\varphi) = \left(\frac{Y_{\text{reading}}(\varepsilon,\varphi)}{<Y_{\text{reading}}(\varepsilon)>} - 1 \right) \cdot 100\%$$

where

$Y_{\text{reading}}(\varepsilon,\varphi)$ is the reading of the radiometer at angles ε and φ

$<Y_{\text{reading}}(\varepsilon)>$ is the average response at incidence angle ε defined by:

$$<Y_{\text{reading}}(\varepsilon)> = \frac{\sum\limits_{i=1}^{n} Y_{\text{reading}}(\varepsilon,\varphi_i)}{n}$$

$Y_{\text{reading}}(\varepsilon,\varphi)$ is measured at n discrete azimuth angles φ_i with 1<=i<=n at incidence angle ε. The angular response should be measured at least at four different azimuth angles (e.g., 0°,90°,180°, and 270°).

Biologically effective irradiance; biological weighting function
A biological weighting function describes the wavelength dependence of effects introduced by electromagnetic radiation on biological matter. Depending on the effect and the involved organism different biological weighting functions $W(\lambda)$ are used. The biologically effective irradiance $E_{weighted}$ is calculated by multiplying global spectral irradiance $E_G(\lambda)$ with the action spectrum $W(\lambda)$ and integrating over wavelength λ:

$$E_{weighted} = \int E_G(\lambda) \cdot W(\lambda)\, d\lambda$$

An important weighting function is the action spectrum for erythema proposed by *CIE* [McKinlay and Diffey, 1987], which describes the wavelength dependence of the reddening of human skin by UV radiation (see also below 'erythemally weighted irradiance E_{CIE}').

Centroid wavelength
The centroid wavelength λ_C of a response function $R(\lambda)$ is defined as defined as follows:

$$\lambda_C = \frac{\int \lambda R(\lambda)\, d\lambda}{\int R(\lambda)\, d\lambda}$$

Cosine error

The deviation of the angular response of a radiometer from the ideal cosine response is specified with two parameters in this document. The first of these (a) is defined according to CIE [1982] and is expressed by the quantity $f_{2a}(\varepsilon, \varphi)$:

$$f_{2a}(\varepsilon, \varphi) = \left(\frac{Y_{\text{reading}}(\varepsilon, \varphi)}{Y_{\text{reading}}(\varepsilon = 0°, \varphi)\ \cos(\varepsilon)} - 1 \right) \times 100\%$$

where ε is the incidence angle of the radiation,

        φ is the azimuth angle,

        $Y_{\text{reading}}(\varepsilon, \varphi)$ is the reading of the radiometer at ε and φ,

        $Y_{\text{reading}}(\varepsilon = 0°, \varphi)\ \cos(\varepsilon)$ is the ideal response.

The second specification (b) refers to isotropic radiation and is defined as follows:

$$f_{2b}(\varepsilon, \varphi) = \left(\frac{\int_0^{2\pi} \int_0^{\pi/2} Y_{\text{reading}}(\varepsilon, \varphi) / Y_{\text{reading}}(\varepsilon = 0°, \varphi)\ \sin(\varepsilon)\ d\varepsilon\ d\varphi}{\int_0^{2\pi} \int_0^{\pi/2} \cos(\varepsilon)\ \sin(\varepsilon)\ d\varepsilon\ d\varphi} - 1 \right) \times 100\%$$

Detection threshold

Minimum irradiance that is detectable.

Erythemally weighted irradiance E_{CIE}

Global spectral irradiance $E_G(\lambda)$ multiplied with the action spectrum for erythema, $C(\lambda)$, proposed by CIE [McKinlay and Diffey, 1987], and integrated over wavelength λ:

$$E_{CIE} = \int_{250\text{nm}}^{400\text{nm}} E_G(\lambda) \cdot C(\lambda) d\lambda$$

where $C(\lambda)$ = 1   for $250 < \lambda \le 298$ nm

                = $10^{(0.094(298-\lambda))}$ for $298 < \lambda \le 328$ nm

                = $10^{(0.015(139-\lambda))}$ for $328 < \lambda \le 400$ nm

Global spectral irradiance $E_G(\lambda)$

Radiant energy dQ arriving per time interval dt, per wavelength interval $d\lambda$, and per area dA on a horizontal surface from all parts of the sky above the horizontal, including the disc of the sun itself:

$$E_G(\lambda) = \frac{dQ}{dt dA d\lambda} = E_D(\lambda) \cdot \cos(\psi) + E_S(\lambda); \qquad \text{(units: W m}^{-2}\text{ nm}^{-1}\text{ s}^{-1}\text{)}$$

where ψ is the solar zenith angle,

        $E_D(\lambda)$ is direct normal spectral irradiance, i.e. radiant energy dQ arriving from the disk of the sun per time interval dt, per wavelength interval $d\lambda$, and per area dA on a surface normal to the solar beam and

        $E_S(\lambda)$ is diffuse spectral irradiance, i.e. radiant energy dQ arriving per time interval dt, per wavelength interval $d\lambda$, and per area dA on a horizontally oriented surface from all parts of the sky above the horizontal, **excluding** the disc of the sun.

Linearity

The linearity of a radiometer is the degree to which the output quantity of the radiometer (e.g., a voltage) is proportional to the input quantity (e.g., global spectral irradiance).

Response-weighted-irradiance

Response-weighted irradiance E_W is defined in this document as the integral of the product of spectral irradiance $E(\lambda)$ and the spectral response function $R_i(\lambda)$ of channel i from a multi-filter radiometer:

$$E_W = \int_0^\infty R_i(\lambda)E(\lambda)d\lambda$$

Spectral sensitivity or spectral response function $R(\lambda)$

Ratio of the signal from a specific channel of a filter radiometer output, $dV(\lambda)$, to the spectral irradiance $dE(\lambda)$ at the place of the radiometer's collector, as a function of wavelength λ:

$$R(\lambda) = \frac{dV(\lambda)}{dE(\lambda)}$$

Remarks:
   a) For measuring $R(\lambda)$, a tunable radiation source is required. A system for measuring $R(\lambda)$ is described in Section 5.1.
   b) In this document $R(\lambda)$ is regarded a relative function and can be multiplied with a wavelength independent factor.

Spectroradiometer

Instrument for the spectrally resolved measurement of electromagnetic radiation. Instruments of this type are described in Part 1 of this document series [Seckmeyer et al., 2001].

Total ozone column

Height of a hypothetical layer which would result if all ozone molecules in a vertical column above the Earth's surface were brought to standard pressure (1013.25 hPa) and temperature (273.15 K). The total ozone column is usually reported in milli-atmosphere-centimeters (m-atm-cm), commonly called 'Dobson units' (DU).). The global average ozone amount is close to 300 DU, which corresponds to a layer of thickness 3 mm at STP.

One DU
   • Defines the amount of ozone in a vertical column which, when reduced to standard pressure and temperature, will occupy a depth of 0.01 mm.
   • Corresponds to $2.69 \cdot 10^{16}$ molecules/cm².

UV-A radiation

Electromagnetic radiation between 315 and 400 nm.

UV-B radiation

Electromagnetic radiation between 280 and 315 nm.

———

REFERENCES

Bais A.F., S. Kazadzis, D. Balis, C. S. Zerefos, and M. Blumthaler. (1998). Correcting global solar UV spectra recorded by a Brewer spectroradiometer for its angular response error, Appl. Opt., 37(27). 6339 - 6344.

Bernhard G. and G. Seckmeyer. (1997). New entrance optics for solar spectral UV measurements, Photochem. and Photobiol., 65(6), 923-930.

Bernhard, G., C. R. Booth, and J. C. Ehramjian. (2005). Real-time ultraviolet and column ozone from multichannel ultraviolet radiometers deployed in the National Science Foundation's ultraviolet monitoring network. Optical Engineering, 44(4), 041011-1 - 041011-12.

Bernhard, G., C. R. Booth, and J. C. Ehramjian. (2008). Comparison of UV irradiance measurements at Summit, Greenland; Barrow, Alaska; and South Pole, Antarctica, Atmos. Chem. Phys., 8(16), 4799–4810.

Bigelow, D. S. and J. R. Slusser. (2000). Establishing the stability of multi-filter UV rotating shadow-band radiometers, J. Geophys. Res.,105(D4), 4833-4840.

Blumthaler M., J. Gröbner, M. Huber, and W. Ambach. (1996). Measuring spectral and spatial variations of UVA and UVB sky radiance, Geophys. Res. Lett., 23(5), 547-550.

Bolsée, D., A. R. Webb, D. Gillotay, B. Dörschel, P. Knuschke, A. Krins, and I. Terenetskaya. (2000). Laboratory Facilities and Recommendations for the characterization of Biological Ultraviolet Dosimeters, Appl. Opt. 39(16), 2813-2822.

Booth, C. R., Synthetic UV spectroradiometry. (1997). in: IRS'96 Current Problems in Atmospheric Radiation, Eds. W.L. Smith and K. Stamnes, Deepak Publ. Hampton, Virginia, U.S.A., pp. 849-852.

Commission International de l'Éclairage (CIE) (Eds.). (1982). Methods of characterising the performance of radiometers and photometers, CIE publication, No 53 (TC-2.2), Paris, France.

Cordero R. R., G. Seckmeyer G., and F. Labbe. (2008). Cosine error influence on ground-based spectral UV irradiance measurements, Metrologia, 45, 406-414.

Dahlback, A. (1996). Measurements of biologically effective UV doses, total ozone abundances, and cloud effects with multichannel, moderate bandwidth filter instruments, Appl. Opt., 35(33), 6514-6521.

Davis, J. M. and J. Slusser (2005). New USDA UVB synthetic spectra algorithm, in: Ultraviolet Ground- and Space-based Measurements, Models, and Effects V, edited by G. Bernhard, J. R. Slusser, J.R. Herman, and W. Gao, Proceedings of SPIE, Vol. 5886, page 0B-1 - 0B-7.

Diaz, S. C. R. Booth, R. Armstrong, C. Brunat, S. Cabrera, C. Camilion, C. Casiccia, G. Deferrari, H. Fuenzalida, C. Lovengreen, A. Paladini, J. Pedroni, A. Rosales, H. Zagarese, and M. Vernet. (2005). Multichannel radiometer calibration: a new approach, Appl. Opt., 44(26), 5374-5380.

di Sarra, A., P. Disterhoft, and J. J. De Luisi. (2002). On the importance of spectra responsivity of Robertson-Berger-type Ultraviolet Radiometers for Long-term Observations, Photochem, Photobiol, 76(1), 64-72.

Feister U., R. Grewe and K. Gericke. (1997). A method for correction of cosine errors in measurements of spectral UV irradiance, Solar Energy, 60(6), 313 - 332.

Feister, U., A. Kaifel, R.-D. Grewe, J. Kaptur, O. Reutter, M. Wohlfart, and K. Gericke (2005). Fast measurements of solar spectral UV irradiance—first performance results of two novel spectroradiometers, Optical Engineering, Volume 44(4), 041007-1 - 041007-9.

Fuenzalida, H. A. (1998). Global ultraviolet spectra derived directly from observations with multichannel radiometers, Appl. Opt., 37(33), 7912-7919.

Gao, W., J. R. Slusser, L. C. Harrison, P. Disterhoft, Q. Min, B. Olson, K. Lantz and B. Davis. (2002). Comparisons of UV Synthetic Spectra Retrieved from the USDA UV Multi-filter Rotating Shadow-band Radiometer with Collocated USDA Reference UV Spectroradiometer and NIWA UV Spectroradiometer, in: Ultraviolet Ground- and Space-based Measurements, Models, and Effects, edited by J.R. Slusser, J.R. Herman, and W. Gao, Proceedings of SPIE, Vol. 4482, 408-414.

Grenfell, T. C., S. G. Warren, and P. C. Mullen. (1994). Reflection of solar radiation by the Antarctic snow surface at ultraviolet, visible, and near infrared wavelengths, J. Geophys. Res., 99(D9), 18,669–18,684.

Gröbner J., M. Blumthaler, W. Ambach. (1996). Experimental investigation of spectral global irradiance measurement errors due to non ideal cosine response, Geophys. Res. Lett., 23(18), 2493-2496.

Harrison, L., J. J. Michalsky, and J. Berndt. (1994a). Automated multifilter rotating shadow-band radiometer: an instrument for optical depth and radiation measurements, Appl. Opt., 33(22), 5118-5121.

Harrison L. and J. Michalsky (1994b). Objective algorithms for the retrieval of optical depths from ground based measurements, Appl. Opt., 33, 5126-5132.

Hofmann, D. J., S. J. Oltmans, G. L. Koenig, B. A. Bodhaine, J. M. Harris, J. A. Lathrop, R. C. Schnell, J. Barnes, J. Chin, D. Kuniyuki, S. Ryan, R. Uchida, A. Yoshinaga, P. J. Neale, D. R. Hayes, J., V. R. Goodrich, W. D. Komhyr, R. D. Evans, B. J. Johnson, D. M.Quincy, and M. Clark. (1996). Record low ozone at Mauna Loa Observatory during winter 1994-1995: a consequence of chemical and dynamical synergism?, Geophys. Res. Lett., 23 (12), 1533-1536.

Hülsen G. and J. Gröbner. (2007). Characterization and calibration of ultraviolet broadband radiometers measuring erythemally weighted irradiance, Appl. Opt. 46(23), 5877-5886.

Janson, G. T. and J. R. Slusser. (2003). Long-term stability of UV multifilter rotating shadowband radiometers, in: Ultraviolet Ground- and Space-based Measurements, Models, and Effects III, edited by J. R. Slusser, J. R. Herman, and W. Gao, Proceedings of SPIE, Vol. 5156, 94-100.

Janson, G., J. Slusser, G. Scott, P. Disterhoft, K. Lantz. (2004). Long-term stability of UV multi-filter rotating shadowband radiometers, Part 2: lamp calibrations versus the Langley method, in: Ultraviolet Ground and Space-based Measurements Models, and Effects IV, edited by J. R. Slusser, J. R. Herman, W. Gao, and G. Bernhard, Proceedings of SPIE, Vol. 5545, 43-48.

Johnsen, B. J., O. Mikkelborg, M. Hannevik, L. T. Nilsen, G. Saxebøl, and K. G. Blaasaas. (2002). The Norwegian UV monitoring programme. Period 1995/96 to 2001, Strålevern Rapport 2002:4, Norwegian Radiation Protection Authority.

Johnsen, B., B. Kjeldstad, T. N. Aalerud, L. T. Nilsen, J. Schreder, M. Blumthaler, G. Bernhard, C. Topaloglou, O. Meinander, A. Bagheri, J. R. Slusser, and J. Davis. (2008a). Intercomparison and harmonization of UV Index measurements from multiband filter radiometers, J. Geophys. Res., 113, D15206, doi:10.1029/2007JD009731.

Johnsen, B., Berit Kjeldstad, T. N. Aalerud, L. T. Nilsen, J. Schreder, M. Blumthaler, G. Bernhard, C. Topaloglou, O. Meinander, A. Bagheri, J. R. Slusser and J. Davis. (2008b). Intercomparison of global UV index from Multiband filter radiometers: Harmonization of global UVI and spectral irradiance, WMO GAW report no. 179, WMO TD no. 1454, available at
http://www.wmo.int/pages/prog/arep/gaw/documents/GAW179-WEB.pdf

Lantz, K., P. Disterhoft, C. Wilson, G. Janson, J. Slusser, S. Bloms, and J. Michalsky. (2005). Out of Band Rejection Studies of the UV multi-filter rotating shadow-band radiometers, in: Remote Sensing of Clouds and the Atmosphere X, edited by K. Schäfer, A. T. Comerón, J. R. Slusser, R. H. Picard, and M. R. Carleer; Proceedings of SPIE, Vol. 5979, 59791N-1.

Liley, J.B., and R.L. McKenzie. (2006). Where on Earth has the highest UV?, in: UV Radiation and its Effects: an update, pp. 26-37, available at
http://www.niwascience.co.nz/rc/atmos/uvconference

Lucas RM, McMichael AJ, Armstrong BK, Smith WT. (2008) Estimating the global disease burden due to ultraviolet radiation exposure. International Journal of Epidemiology; 37 (3): 654-667.

Madronich, S., and S. Flocke. (1995). Theoretical estimation of biologically effective UV radiation at the earth's surface, in Solar Ultraviolet Radiation. NATO, Series I: Advanced Study Institute, edited by C.S. Zerefos, and A.F. Bais, pp. 23-48, Springer, Berlin.

Mayer B. and A. Kylling. (2005). Technical Note: The libRadtran software package for radiative transfer calculations: description and examples of use. Atmos. Chem. Phys., 5(7), 1855-1877.

McKenzie R. L., P. V. Johnston, M. Kotkamp, A. Bittar, J. D. Hamlin. (1992). Solar ultraviolet spectroradiometry in New Zealand: instrumentation and sample results from 1990, Appl. Opt., 31(30), 6501-6509.

McKinlay, A. F., and B. L. Diffey (Eds.) (1987). A reference action spectrum for ultraviolet induced erythema in human skin, CIE J., 6(1), 17–22.

Min, Q. and L. Harrison. (1998). Synthetic spectra for terrestrial ultraviolet measurements, J. Geophys. Res., 103(D14), 17033-17039.

Schmid, B. and C. Wehrli. (1995). Comparison of Sun photometer calibrations by use of the Langley technique and the standard lamp, Appl. Opt., 34(21), 4500-4512.

Schmid B., P. R. Spyak, S. F. Biggar, C. Wehrli, J. Sekler, T. Ingold, C. Maetzler, and N. Kaempfer. (1998). Evaluation of the applicability of solar and lamp radiometric calibrations of a precision Sun photometer operating between 300 and 1025 nm, Appl. Opt., 37(18), 3923-3941.

Schwander H., Mayer B., Ruggaber A., Albold A., Seckmeyer G., Koepke P. (1999). Method to determine snow albedo values in the UV for radiative transfer modelling, Appl. Opt., 38(18), pp 3869-3875.

Schwander, H., A. Kaifel, A. Ruggaber, and P. Koepke. (2001). Spectral radiative-transfer modelling with minimized computation time by use of a neural-network technique, Appl. Opt., 40(3), 331-335.

Seckmeyer G. and G. Bernhard. (1993). Cosine error correction of spectral UV-irradiances, in: Atmospheric Radiation, edited by Knut H. Stamnes, Proceedings, SPIE, 2049, 140-151.

Seckmeyer, G., A. Bais, G. Bernhard, M. Blumthaler, C. R. Booth, P. Disterhoft, P. Eriksen, R. L. McKenzie, M. Miyauchi, and C. Roy. (2001). Instruments to measure solar ultraviolet radiation. Part 1: Spectral instruments, World Meteorological Organization, Global Atmosphere Watch Publication No. 125, WMO TD No. 1066, Geneva, Switzerland.

Seckmeyer, G., A. Bais, G. Bernhard, M. Blumthaler, C. R. Booth, K. Lantz, and R. L. McKenzie. (2005). Instruments to measure solar ultraviolet radiation. Part 2: Broadband instrument measuring erythemally weighted solar irradiance, World Meteorological Organization, Global Atmosphere Watch Publication No. 164, WMO TD No. 1289, Geneva, Switzerland.

Slusser, J. R., J. H. Gibson, D. S. Bigelow, D. Kolinski, W. Mou, G. Koenig, and A. Beaubien. (1999). Comparison of column ozone retrievals employing a UV multi-filter rotating shadow-band radiometer with those from Brewer and Dobson spectrophotometers, Appl. Opt., 38(9), 1543-1551.

Slusser, J. R., J. H. Gibson, D. Kolinski, P. Disterhoft, K. Lantz and A. F. Beaubien. (2000). Langley Method of Calibrating UV Filter Radiometers, J. Geophys. Res., 105(D4), 4841-4849.

Stamnes K., J. R. Slusser, and M. Bowen. (1991). Derivation of total ozone abundance and cloud effects from spectral irradiance measurements. Appl. Opt., 30(30), 4418-4426.

Thorseth, T. M. and B. Kjeldstad. (1999). All-weather ultraviolet solar spectra retrieved at a 0.5 Hz sampling rate, Appl. Opt., 38(30), 6247-6252.

Thorseth T. M., B. Kjeldstad, and B. Johnsen. (2000). Comparison of solar ultraviolet measurements performed with spectroradiometers and moderate bandwidth multichannel radiometers for different cloud conditions, J. Geophys, Res., 105 (D4), 4809-4820.

Webb, A. R., B. G. Gardiner, K. Leszczynski, V. Mohnen, P. Johnston, N. Harrison, and D. Bigelow. (1998). Quality assurance in monitoring solar ultraviolet radiation: the state of the art, World Meteorological Organization, Global Atmosphere Watch Publication No. 146, WMO TD No. 1180, Geneva, Switzerland.

Webb, A. R., B. G. Gardiner, T. J. Martin, K. Leszczynski, J. Metzdorf, and V. A. Mohnen. (2003). Guidelines for site quality control of UV monitoring, World Meteorological Organization, Global Atmosphere Watch Publication No. 126, WMO TD No. 884, Geneva, Switzerland.

Weihs P., J. Lenoble, M. Blumthaler, T. Martin, G. Seckmeyer, R. Philipona, de la Casiniere, C. Sergent, J. Gröbner, T. Cabot, D. Masserot, T. Pichler, E. Pougatch, G. Rengarajan, D. Schmucki, and S. Simic. (2001). Modelling the effect on an inhomogeneous surface albedo on incident UV radiation in mountainous terrain: determination of an effective surface albedo, Geophys. Res. Lett., 28(16), 3111-3114.

WHO (2008) World Health Organization, International Agency for Research on Cancer. Vitamin D and cancer. IARC Working Group Reports, *WHO Press*, **5**, 148.

WMO (1986). Recent progress in sun photometry; Determination of the aerosol optical depth, Environmental Pollution Monitoring and Research Programme 43, WMO TD No.143, Geneva, Switzerland.

WMO (1993). Report of the WMO workshop on the measurement of atmospheric optical depth and turbidity. Silver Spring, Md., 6-10 December, (B. Hicks, ed.) Global Atmosphere Watch Publication No. 101, WMO TD 659, Geneva, Switzerland.

Wuttke S., G. Seckmeyer, and G. Koenig-Langlo. (2006). Measurements of spectral snow albedo at Neumayer, Antarctica, Annales Geophysicae, 24, 7-21.

———

Centre Wavelengths of some Available Multi-Filter Instruments

Instruments to measure global irradiance
- Biospherical Instruments GUV: 305, 313, 320, 340, 380, 395 (all 10 nm fwhm), PAR.
- NILU-UV: 300, 312, 320, 340, 380, (all 10 nm fwhm), PAR.
- UV-SPRAFIMO: 303.5, 309, 314.5, 327, 387, (all ~2nm).

Instruments equipped with shadowbands measuring global and diffuse irradiance
- Yankee-SPUV: 300, 311, 317, 325, 332, 368, 500, 673, 778, 870.
- Yankee UV-MFRSR: 300, 305.5, 311.5, 317.5, 325, 332.5, 368 (all 2 nm fwhm, partly Dobson wavelengths).
- Yankee MFRSR: 415, 500, 615, 673, 870, 940 (all 10 nm fwhm).

Instruments mounted on a solar tracker for measuring direct irradiance
- UV-PFR: 305, 311, 318, 332 (all 1,5 nm fwhm), optional 368, 412, 500, 862.
- CIMEL sunphotometer: 440, 670, 870, 936,1020 (10 nm fwhm).
- SPM-2000 Sun photometer 300, 313, 305, 310, 320, 340, 368, 412, 450, 500, 610, 675, 719, 778, 817, 862, 946, 1024 [Schmidt et al., 1998].

Wavelength for total ozone derivation
- Dobson wavelengths: A (305.5, 325.4), B (308.8, 329.1), C (311.45, 332.4), D (317.66, 339.8).
- Brewer wavelengths: 306.3, 310.1, 313.5, 316.8, 320.
- Ozone derivation from global spectra suggested by Stamnes et al. [1991]: 305, 340.

Wavelengths frequently used for specific applications
- Column waver vapour retrieval: 940 nm.
- Atmospheric aerosol optical depth measurements: 368, 412, 450, 500, 610, 675, 719, 778, 817, 862, 946, 1024 nm. Wavelength recommended by [WMO, 1986; WMO, 1993].
- Wavelength affected by NO_2 and SO_2 absorption.

_____

References of Freely Available Radiative Transfer Programmes

libRadtran - Library for Radiative Transfer
http://www.libradtran.org

TUV - Tropospheric Ultraviolet and Visible Radiation Model
http://www.acd.ucar.edu/TUV/

STAR - System for Transfer of Atmospheric Radiation
http://www.meteo.physik.uni-muenchen.de/strahlung/uvrad/Star/STARinfo.htm

FASTRT - Fast radiation transfer modelling
(Online radiative transfer model based on Look-Up Tables that were calculated with libRadtran.)
http://zardoz.nilu.no/~olaeng/fastrt/fastrt.html

SBDART - Santa Barbara DISORT Atmospheric Radiative Transfer Model
http://www.ncgia.ucsb.edu/projects/metadata/standard/uses/sbdart.htm

Additional codes may be found here:
http://en.wikipedia.org/wiki/List_of_atmospheric_radiative_transfer_codes

———

Calculations in Support of Specifications Provided in Section 3

Calculations presented in this Annex explore the magnitude of measurement errors resulting from:

- Wavelength-shifts of spectral response functions.
- Changes in the bandwidth of spectral response functions.
- Systematic errors that may occur when multi-filter instruments are calibrated with lamps.
- Light leakage (i.e. significant response outside the filter bandwidth).

Calculations are based on modelled solar clear sky UV spectra, E_s, generated by the libRadtran radiative transfer software package [Mayer and Kylling, 2005]. Input parameters are total ozone O_3, SZA θ, surface albedo (set to 5%), and default aerosol amount.

A set of idealized, rectangular spectral response functions are used. These functions have unity response within the fwhm, and a base level of 10^{-10} ('zero') outside this range.

C.1 Effects from wavelength-shifts of spectral response functions

Calculations of relative errors in the signal resulting from wavelength-shifts of spectral response functions are based on the following equation.

$$\Delta U_i(\lambda, \delta\lambda, FWHM) = \left(\frac{\int R_i(\lambda + \partial\lambda, fwhm, \lambda') E_S(\lambda', \theta, O_3) d\lambda'}{\int R_i(\lambda, fwhm, \lambda') E_S(\lambda', \theta, O_3) d\lambda'} - 1 \right) \cdot 100\%$$

Here $\Delta U_i(\lambda, \delta\lambda, FWHM)$ is the relative change in signal at nominal wavelength λ, for a small wavelength error δλ, and a given bandwidth expressed in fwhm, and R_i is the spectral response function of channel i.

Results corresponding to a wavelength shift of δλ = 0.03 nm at the nominal centre wavelength of λ = 305 nm and fwhm = 10.0 nm are shown in Figure C.1. Errors are smaller than 2% for SZA less than 80º and ozone amounts between 250 DU and 450 DU. Errors in the signal diminish with longer centre wavelengths but are almost independent of fwhm for bandwidths between 1.0 nm and 10 nm fwhm.
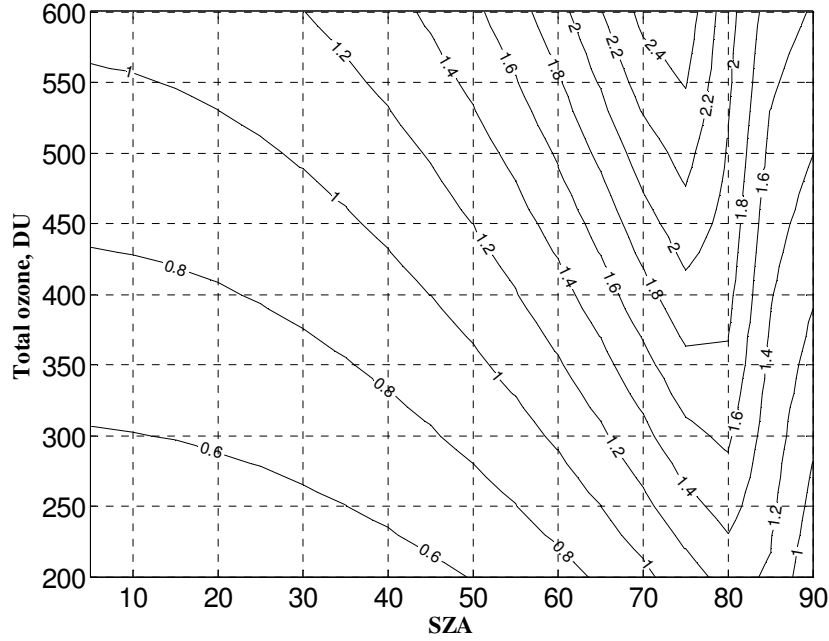
Figure C.1 - Contour diagram of % errors in the signal from a 0.03 nm shift for nominal centre wavelength at 305 nm, a bandwidth of 10.0 nm fwhm, as function of SZA and total ozone amount. Contour numbers are given in percent.

C.2 Effects from changes in bandwidth

Errors from shifts in bandwidth are based on the equation below, where the bandwidth is expressed as fwhm and modified with a constant δ.

$$\Delta U_i(\lambda, FWHM, \delta) = \left(\frac{\int R_i(\lambda, \lambda', FWHM \cdot (1-\delta)) \cdot E_S(\lambda', \theta, O_3) d\lambda'}{\int R_i(\lambda, \lambda', FWHM) \cdot E_S(\lambda', \theta, O_3) d\lambda'} - 1 \right) \cdot 100\%$$

Results are normalized to SZA = 40º and total ozone of 300 DU in order to focus on the relative changes as function of SZA and O_3.

Errors resulting from a 2% change in fwhm at centre wavelength of λ = 305 nm and a nominal bandwidth of 10.0 nm fwhm can be as high as 3% for typical ozone amounts and SZA less than 80º (Figure C.2). Similar calculations for a nominal bandwidth of 2.0 nm result in very small errors (Figure C.3). Errors are wavelength dependent. At UV-B wavelengths in the ozone cut-off region, the errors become increasingly larger with shorter centre wavelengths, whereas the effect is insignificant outside the ozone cut-off region.

Difference [%] induced by 0.02 [%] variation in FWHM
Center wavelength 305.0nm, FWHM 10.0nm, total Ozone 250 to 450 DU

Figure C.2 - Difference in signal at 305 nm for 2% variations in bandwidth, calculated for a bandwidth of 10.0 nm fwhm. Differences are relative to SZA 40º and total ozone 300 DU.

Difference [%] induced by 0.02 [%] variation in FWHM
Center wavelength 305.0nm, FWHM 2.0nm, total Ozone 250 to 450 DU

Figure C.3 - Same as Figure C.2 but calculated for a bandwidth of 2.0 nm fwhm.
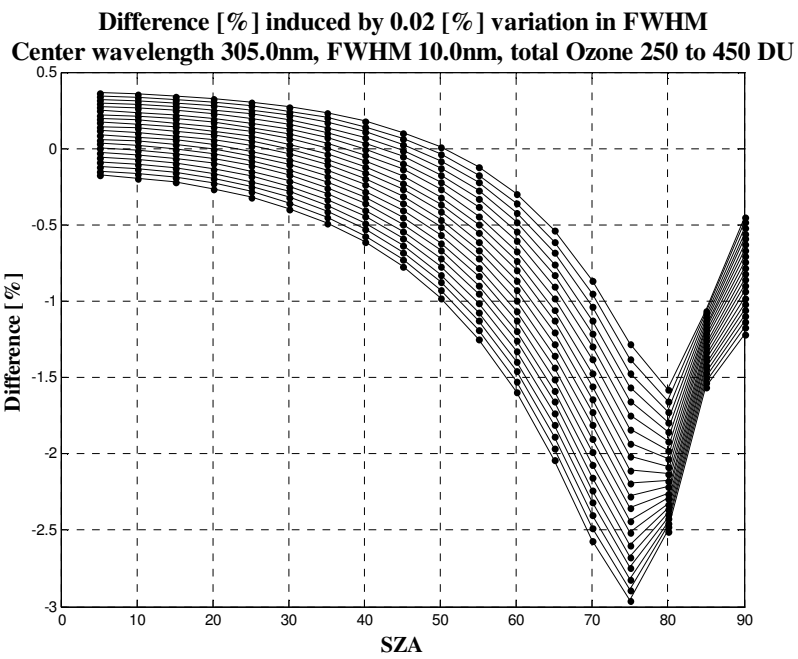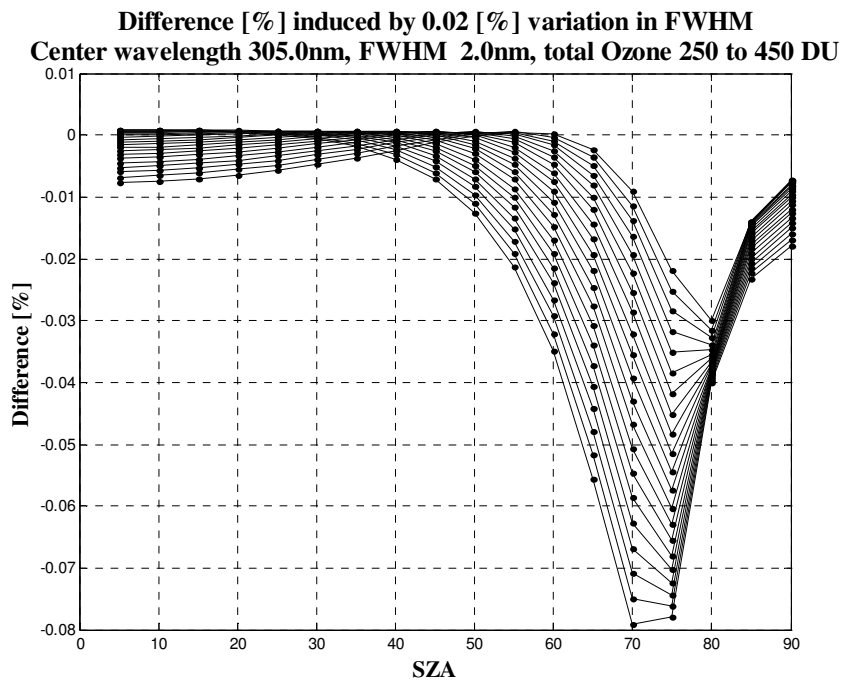
C.3 Systematic errors resulting from calibrating multi-filter instruments with a standard of spectral irradiance

If multi-filter instruments are calibrated with a Standard of Spectral Irradiance (Section 4.1.3) the correction function $K_i^{(3)}$ must be applied to account for the mismatch of the solar spectrum and the spectrum of the standard lamp. If this correction function is not applied as described in Section 4, large errors in the measured solar irradiance will result. These errors can be expressed by the error function $\Delta U(\lambda, FWHM, \theta, O_3)$:

$$\Delta U(\lambda, FWHM, \theta, O_3) = \left(\frac{E_{S,i,approx(\lambda)}}{E_{S,i,complete(\lambda, FWHM, \theta, O_3)}} - 1 \right) \cdot 100\%$$

$$= \left(\frac{E_L(\lambda)}{E_S(\lambda, \theta, O_3)} \cdot \frac{\int R_i(\lambda', FWHM) E_S(\lambda', \theta, O_3) d\lambda'}{\int R_i(\lambda', FWHM) E_L(\lambda') d\lambda'} - 1 \right) \cdot 100\%$$

Figures C.4 and Figure C.5 show $\Delta U(\lambda, FWHM, \theta, O_3)$ as a function of SZA for a centre wavelength of 305 nm and bandwidths of 10.0 nm and 1.0 nm, respectively. Data shown in both figures are normalized to one for SZA = 40º and total ozone of 300 DU. For a hypothetical instrument with a bandwidth of 10 nm, the error can be as large as 200% for a filter centred at 305 nm (Figure C.4). However, it is less than 1.2% for an instrument with a filter centred at 305 nm with a bandwidth of 1.0 nm (Figure C.5).

If a correction function is applied to the calibration using a lamp Standard of Spectral Irradiance as described in Section 4, the % errors in the signal will be significantly less. Because the correction function includes the spectral response function, errors or changes in the wavelength and the bandwidth as described in Sections C.1 and C.2 will propagate to the correction function.

Difference [%] solar to lamp based calibration factors at nominally 305nm
FWHM 10.0nm, total ozone 250-450 DU

Figure C.4 - Error $\Delta U(\lambda, FWHM, \theta, O_3)$ for λ = 305 nm and FWHM = 10 nm. Differences are relative to SZA 40º and total ozone 300 DU. Errors for total ozone of 250 DU (450 DU) are indicated by the bottom (top) function. The graph indicates that measurements of spectral irradiance at 305 nm can be in error by as much as 200% if a multi-filter instrument with a bandwidth of 10 nm is calibrated with a standard lamp, and no corrections are applied.

34

Difference [%] solar to lamp based calibration factors at nominally 305nm
FWHM 1.0nm, total ozone 250-450 DU
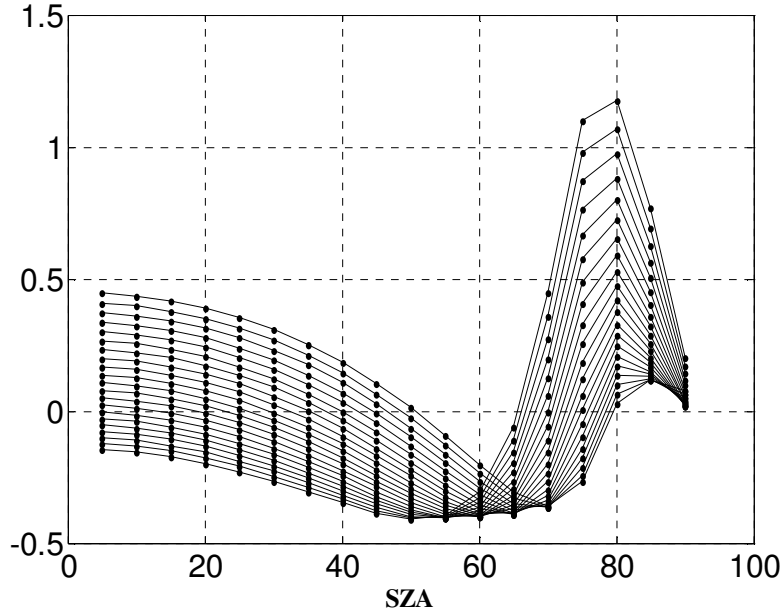
Figure C.5 - Same as Figure C.4, but for a bandwidth of 1.0 nm FWHM.
The maximum error is less than ±1.2%.

C.4 Errors from stray light (light leakage) in spectral response functions

The sensitivity of multi-channel filter radiometer to radiation outside the core wavelength range of their spectral response functions can lead to considerable errors. These errors are quantified here with the function $\Delta U_i(\lambda, FWHM, Tail)$, defined as:

$$\Delta U_i(\lambda, FWHM, Tail) = \left(\frac{\int R_i(\lambda, \lambda', FWHM, Tail) E_S(\lambda', \theta, O_3) d\lambda'}{\int R_i(\lambda, \lambda' FWHM, NoTail) E_S(\lambda', \theta, O_3) d\lambda'} - 1 \right) \cdot 100\%$$

The parameter "NoTail" is equal to 10^{-10}, which for all practical purposes is identical to zero, and the parameter "Tail," which is set to 10^{-4}. (This means that the instrument channel in question has a wavelength-independent sensitivity of 10^{-4} across the UV band relative to the peak sensitivity of the spectral response function.) Figures C.6 and Figure C.7 show $\Delta U_i(\lambda, FWHM, Tail)$ as a function of SZA for a centre wavelength of 305 nm and bandwidths of 10.0 nm and 1.0 nm, respectively. For a hypothetical instrument with a bandwidth of 10 nm, the error may be as high as 80% for large SZA, but is below 5% for SZA smaller than 55°. For an instrument with a bandwidth of 1.0 nm, the error can be as large as 1500% (Figure C.7). This indicates that light leakage can be an important error source for filter instruments with small bandwidth.

Difference [%] induced by secondary peak of magnitude 1E-004
Center wavelength 305.0nm, FWHM 10.0nm, total Ozone 250 to 450 DU

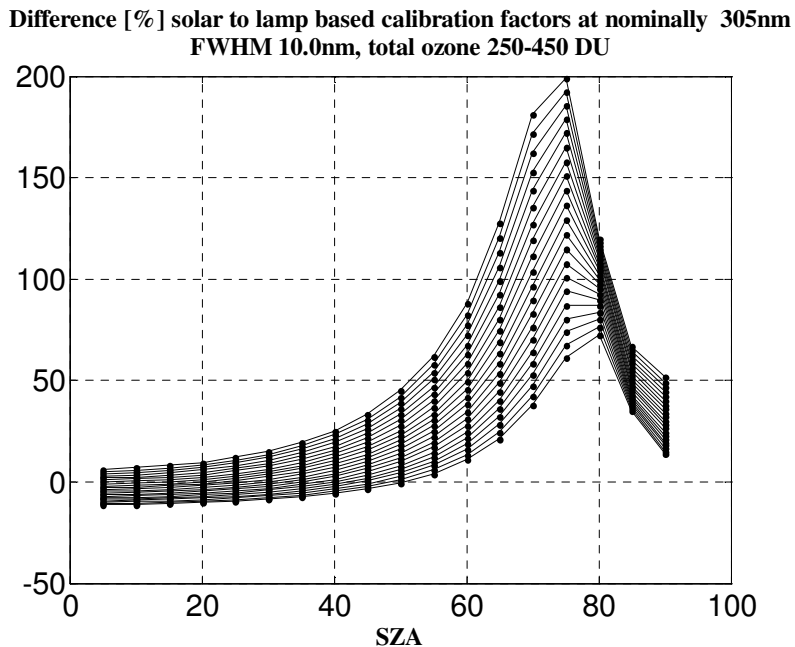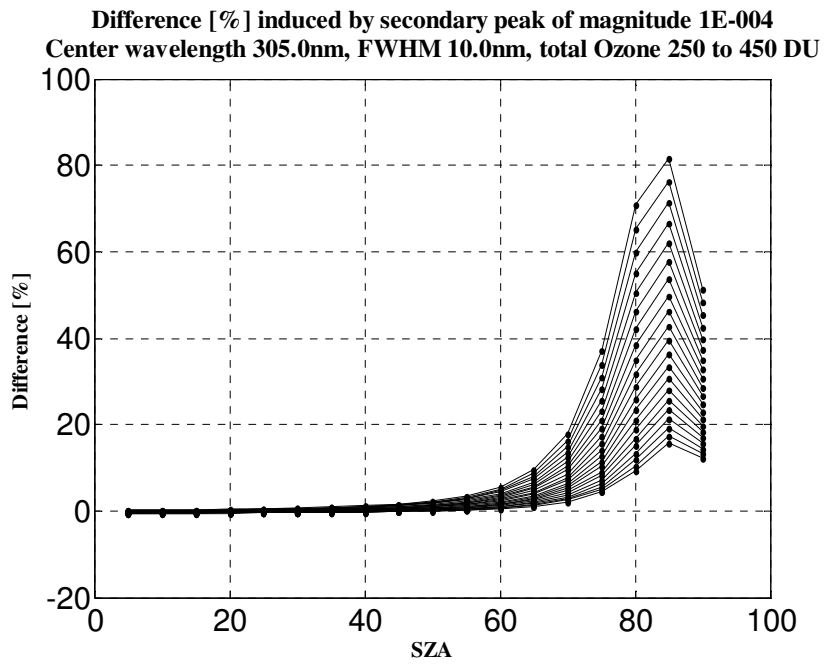Figure C.6 - Error $\Delta U_i(\lambda, FWHM, Tail)$ for λ = 305 nm and FWHM= 10 nm. Differences are relative to SZA 40º and total ozone 300 DU. Errors for total ozone of 250 DU (450 DU) are indicated by the bottom (top) function. The graph indicates that measurements of spectral irradiance at 305 nm can be in error by up to 80% if a multi-filter instrument with a bandwidth of 10 nm has a wavelength-independent sensitivity of 10^{-4} across the UV band relative to the peak sensitivity of the spectral response function.

Difference [%] induced by secondary peak of magnitude 1E-004
Center wavelength 305.0nm, FWHM 1.0nm, total Ozone 250 to 450 DU
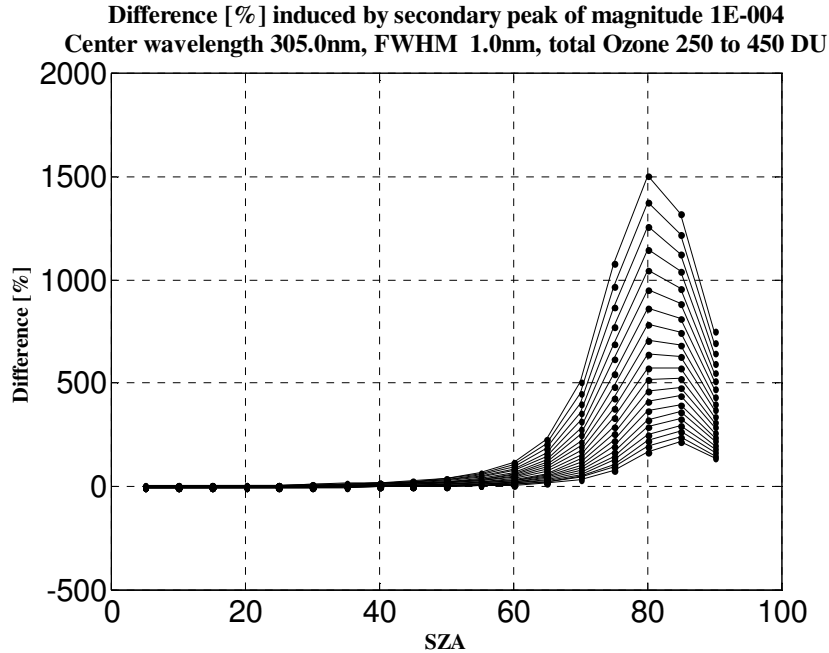
Figure C.7 - Same as Figure C.6, but for a bandwidth of 1.0 nm FWHM. The maximum error is ±1500%.

———————

Maximum Irradiance at the Earth's Surface

The maximum UV irradiance from 20 years of gridded satellite estimations from TOMS instruments corresponds to a UV Index of 24.8, as reported by Liley and McKenzie [2006]. That value occurred in Cusco, Peru (13.5°S, 72°W) in February 1998, when the Sun was directly overhead. The mean altitude of the grid cell (~100 km x 100 km) was 3655 m, though the surrounding terrain extended to altitudes of 6500 m. At the time of this maximum, the total column ozone was 235 DU. Spectral irradiances were calculated with the TUV radiative transfer code [Madronich and Flocke, 1995] to match these conditions. No clouds or aerosols were included, and to simulate the UVI value of 24.8 a surface albedo of 0.8 is used. It should be noted that such high surface albedo are not realistic for this location and season. Effective albedos above 0.8 are realistic only for Antarctica [Grenfell et al., 1994; Schwander et.al., 1999; Weihs et.al., 2001; Wuttke et.al., 2006].

To estimate the maximum spectral irradiances (W m^{-2} nm^{-1}) a calculation was performed for the highest peak in this region (6500 m) with assumption of full snow cover (surface albedo 0.99) and assuming a total column ozone amount of 200 DU; such low ozone values have been observed previously within the tropics. For example the lowest ozone amount measured at Mauna Loa Observatory was 200 DU [Hofmann et al., 1996]. Finally, a further 20% increase was introduced to account for possible enhancements due to clouds that do not obscure the sun.

These spectral irradiances are compared with the extraterrestrial solar spectral irradiance in the figure and table below.
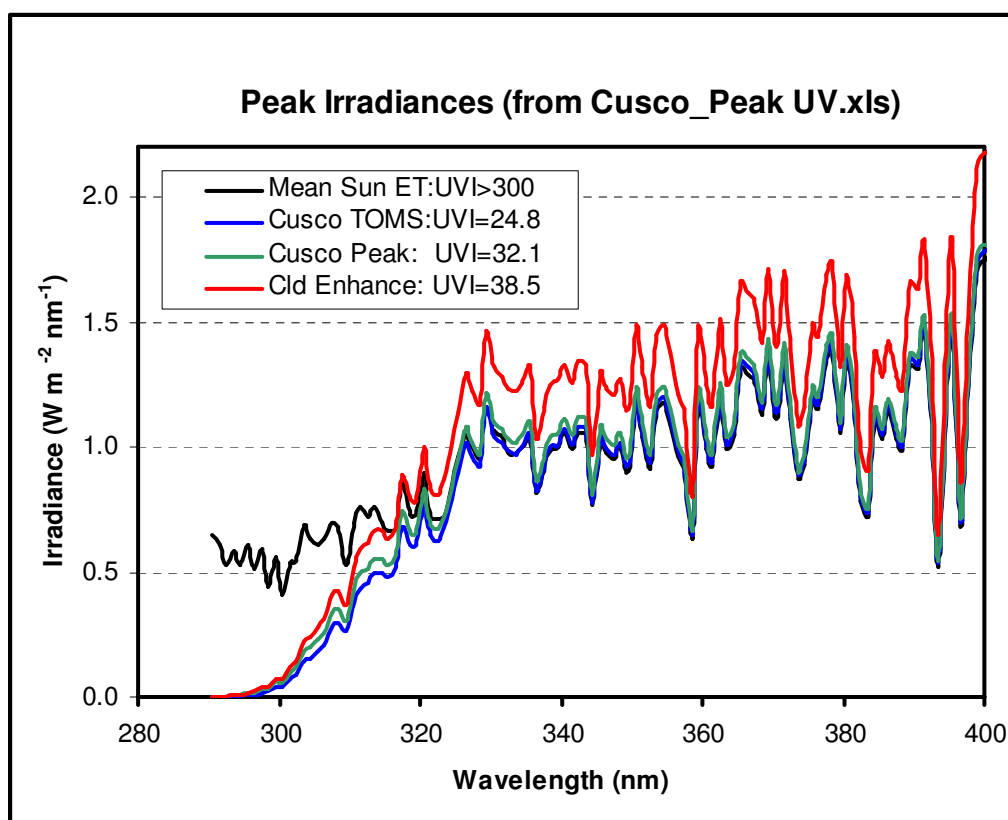
Wvl (nm)	Mean Sun ET: UVI>300	Cusco TOMS UVI=24.8	Cusco Peak UVI=32.1	20% Cloud Enhanced UVI=38.5
290.5	6.48E-01	1.10E-04	4.41E-04	5.29E-04
291.5	6.12E-01	3.26E-04	1.07E-03	1.28E-03
292.5	5.26E-01	6.64E-04	1.91E-03	2.29E-03
293.5	5.83E-01	1.65E-03	4.19E-03	5.03E-03
294.5	5.30E-01	2.75E-03	6.38E-03	7.66E-03
295.5	6.10E-01	6.52E-03	1.36E-02	1.63E-02
296.5	5.16E-01	9.44E-03	1.81E-02	2.17E-02
297.5	5.93E-01	1.85E-02	3.26E-02	3.91E-02
298.5	4.44E-01	2.03E-02	3.38E-02	4.06E-02
299.5	5.64E-01	3.85E-02	6.03E-02	7.24E-02
300.5	4.08E-01	3.84E-02	5.73E-02	6.88E-02
301.5	5.36E-01	6.84E-02	9.74E-02	1.17E-01
302.5	5.47E-01	8.81E-02	1.21E-01	1.45E-01
303.5	6.85E-01	1.41E-01	1.87E-01	2.24E-01
304.5	6.33E-01	1.55E-01	2.00E-01	2.40E-01
305.5	6.11E-01	1.85E-01	2.31E-01	2.77E-01
306.5	6.32E-01	2.11E-01	2.60E-01	3.12E-01
307.5	7.00E-01	2.83E-01	3.39E-01	4.07E-01
308.5	6.77E-01	2.97E-01	3.52E-01	4.22E-01
309.5	5.27E-01	2.61E-01	3.04E-01	3.65E-01
310.5	6.94E-01	3.76E-01	4.32E-01	5.18E-01
311.5	7.59E-01	4.33E-01	4.94E-01	5.93E-01
312.5	7.21E-01	4.57E-01	5.14E-01	6.17E-01
313.5	7.62E-01	4.94E-01	5.53E-01	6.64E-01
314.5	6.99E-01	5.00E-01	5.53E-01	6.64E-01
315.5	6.66E-01	4.79E-01	5.29E-01	6.35E-01
316.5	6.69E-01	5.18E-01	5.67E-01	6.80E-01
317.5	8.66E-01	6.79E-01	7.41E-01	8.89E-01
318.5	7.27E-01	6.10E-01	6.60E-01	7.92E-01
319.5	7.30E-01	6.06E-01	6.56E-01	7.87E-01
320.5	8.94E-01	7.74E-01	8.33E-01	1.00E+00
321.5	7.17E-01	6.45E-01	6.91E-01	8.29E-01
322.5	7.12E-01	6.28E-01	6.73E-01	8.08E-01
323.5	7.24E-01	6.81E-01	7.24E-01	8.69E-01
324.5	8.47E-01	7.94E-01	8.44E-01	1.01E+00
325.5	9.61E-01	8.93E-01	9.49E-01	1.14E+00
326.5	1.05E+00	1.02E+00	1.08E+00	1.30E+00
327.5	1.00E+00	9.61E-01	1.02E+00	1.22E+00
328.5	9.61E-01	9.28E-01	9.80E-01	1.18E+00
329.5	1.16E+00	1.16E+00	1.22E+00	1.46E+00
330.5	1.07E+00	1.04E+00	1.10E+00	1.32E+00
331.5	1.04E+00	1.02E+00	1.07E+00	1.28E+00
332.5	9.79E-01	9.85E-01	1.03E+00	1.24E+00
333.5	9.76E-01	9.70E-01	1.02E+00	1.22E+00
334.5	9.98E-01	1.00E+00	1.05E+00	1.26E+00
335.5	1.04E+00	1.05E+00	1.10E+00	1.32E+00
336.5	8.19E-01	8.25E-01	8.63E-01	1.04E+00
337.5	9.22E-01	9.25E-01	9.67E-01	1.16E+00

338.5	9.83E-01	9.97E-01	1.04E+00	1.25E+00
339.5	9.99E-01	1.01E+00	1.06E+00	1.27E+00
340.5	1.05E+00	1.07E+00	1.11E+00	1.33E+00
341.5	9.94E-01	1.01E+00	1.05E+00	1.26E+00
342.5	1.06E+00	1.08E+00	1.12E+00	1.34E+00
343.5	1.05E+00	1.07E+00	1.11E+00	1.33E+00
344.5	7.65E-01	7.76E-01	8.07E-01	9.68E-01
345.5	1.03E+00	1.04E+00	1.08E+00	1.30E+00
346.5	9.77E-01	9.96E-01	1.03E+00	1.24E+00
347.5	9.53E-01	9.72E-01	1.01E+00	1.21E+00
348.5	1.00E+00	1.02E+00	1.06E+00	1.27E+00
349.5	9.08E-01	9.25E-01	9.59E-01	1.15E+00
350.5	1.17E+00	1.19E+00	1.24E+00	1.49E+00
351.5	1.04E+00	1.06E+00	1.10E+00	1.32E+00
352.5	9.16E-01	9.34E-01	9.66E-01	1.16E+00
353.5	1.15E+00	1.17E+00	1.21E+00	1.45E+00
354.5	1.18E+00	1.20E+00	1.24E+00	1.49E+00
355.5	1.09E+00	1.11E+00	1.15E+00	1.38E+00
356.5	9.62E-01	9.81E-01	1.01E+00	1.21E+00
357.5	9.09E-01	9.27E-01	9.57E-01	1.15E+00
358.5	6.42E-01	6.55E-01	6.75E-01	8.10E-01
359.5	1.17E+00	1.19E+00	1.23E+00	1.48E+00
360.5	9.89E-01	1.01E+00	1.04E+00	1.25E+00
361.5	9.27E-01	9.45E-01	9.74E-01	1.17E+00
362.5	1.20E+00	1.23E+00	1.26E+00	1.51E+00
363.5	9.90E-01	1.01E+00	1.04E+00	1.25E+00
364.5	1.05E+00	1.07E+00	1.10E+00	1.32E+00
365.5	1.32E+00	1.34E+00	1.38E+00	1.66E+00
366.5	1.29E+00	1.32E+00	1.35E+00	1.62E+00
367.5	1.27E+00	1.30E+00	1.33E+00	1.60E+00
368.5	1.13E+00	1.15E+00	1.18E+00	1.42E+00
369.5	1.37E+00	1.39E+00	1.43E+00	1.72E+00
370.5	1.12E+00	1.14E+00	1.17E+00	1.40E+00
371.5	1.35E+00	1.38E+00	1.42E+00	1.70E+00
372.5	1.11E+00	1.13E+00	1.16E+00	1.39E+00
373.5	8.69E-01	8.86E-01	9.08E-01	1.09E+00
374.5	9.25E-01	9.43E-01	9.66E-01	1.16E+00
375.5	1.19E+00	1.21E+00	1.24E+00	1.49E+00
376.5	1.15E+00	1.17E+00	1.20E+00	1.44E+00
377.5	1.35E+00	1.38E+00	1.41E+00	1.69E+00
378.5	1.40E+00	1.42E+00	1.45E+00	1.74E+00
379.5	1.05E+00	1.07E+00	1.10E+00	1.32E+00
380.5	1.35E+00	1.38E+00	1.41E+00	1.69E+00
381.5	1.15E+00	1.17E+00	1.20E+00	1.44E+00
382.5	7.86E-01	8.00E-01	8.18E-01	9.82E-01
383.5	7.28E-01	7.41E-01	7.58E-01	9.10E-01
384.5	1.11E+00	1.13E+00	1.15E+00	1.38E+00
385.5	1.03E+00	1.05E+00	1.07E+00	1.28E+00
386.5	1.15E+00	1.17E+00	1.19E+00	1.43E+00
387.5	1.03E+00	1.05E+00	1.07E+00	1.28E+00
388.5	9.89E-01	1.01E+00	1.03E+00	1.24E+00

389.5	1.33E+00	1.35E+00	1.38E+00	1.66E+00
390.5	1.31E+00	1.33E+00	1.36E+00	1.63E+00
391.5	1.47E+00	1.49E+00	1.52E+00	1.82E+00
392.5	1.03E+00	1.04E+00	1.06E+00	1.27E+00
393.5	5.24E-01	5.33E-01	5.43E-01	6.52E-01
394.5	1.19E+00	1.21E+00	1.23E+00	1.48E+00
395.5	1.47E+00	1.49E+00	1.52E+00	1.82E+00
396.5	6.92E-01	7.03E-01	7.17E-01	8.60E-01
397.5	1.10E+00	1.11E+00	1.13E+00	1.36E+00
398.5	1.63E+00	1.65E+00	1.68E+00	2.02E+00
399.5	1.74E+00	1.77E+00	1.80E+00	2.16E+00
400.5	1.76E+00	1.79E+00	1.82E+00	2.18E+00
401.5	1.88E+00	1.91E+00	1.94E+00	2.33E+00
402.5	1.92E+00	1.95E+00	1.98E+00	2.38E+00
403.5	1.77E+00	1.79E+00	1.83E+00	2.20E+00
404.5	1.72E+00	1.74E+00	1.77E+00	2.12E+00
405.5	1.79E+00	1.82E+00	1.85E+00	2.22E+00
406.5	1.74E+00	1.77E+00	1.80E+00	2.16E+00
407.5	1.66E+00	1.69E+00	1.72E+00	2.06E+00
408.5	1.94E+00	1.97E+00	2.00E+00	2.40E+00
409.5	1.82E+00	1.84E+00	1.87E+00	2.24E+00
410.5	1.61E+00	1.64E+00	1.66E+00	1.99E+00
411.5	1.94E+00	1.97E+00	2.00E+00	2.40E+00
412.5	1.93E+00	1.95E+00	1.98E+00	2.38E+00
413.5	1.89E+00	1.92E+00	1.95E+00	2.34E+00
414.5	1.87E+00	1.89E+00	1.92E+00	2.30E+00
415.5	1.86E+00	1.89E+00	1.92E+00	2.30E+00
416.5	1.99E+00	2.02E+00	2.05E+00	2.46E+00
417.5	1.79E+00	1.81E+00	1.84E+00	2.21E+00
418.5	1.81E+00	1.83E+00	1.86E+00	2.23E+00
419.5	1.83E+00	1.85E+00	1.88E+00	2.26E+00
420.5	1.89E+00	1.91E+00	1.94E+00	2.33E+00
421.5	1.94E+00	1.96E+00	1.99E+00	2.39E+00
422.5	1.72E+00	1.75E+00	1.77E+00	2.12E+00
423.5	1.84E+00	1.87E+00	1.89E+00	2.27E+00
424.5	1.89E+00	1.91E+00	1.94E+00	2.33E+00
425.5	1.83E+00	1.85E+00	1.88E+00	2.26E+00
426.5	1.85E+00	1.87E+00	1.90E+00	2.28E+00
427.5	1.69E+00	1.71E+00	1.73E+00	2.08E+00
428.5	1.71E+00	1.73E+00	1.76E+00	2.11E+00
429.5	1.58E+00	1.60E+00	1.62E+00	1.94E+00
430.5	1.22E+00	1.23E+00	1.25E+00	1.50E+00
431.5	1.81E+00	1.83E+00	1.85E+00	2.22E+00
432.5	1.76E+00	1.78E+00	1.81E+00	2.17E+00
433.5	1.85E+00	1.87E+00	1.89E+00	2.27E+00
434.5	1.78E+00	1.80E+00	1.83E+00	2.20E+00
435.5	1.84E+00	1.86E+00	1.88E+00	2.26E+00
436.5	2.06E+00	2.08E+00	2.11E+00	2.53E+00
437.5	1.92E+00	1.94E+00	1.96E+00	2.35E+00
438.5	1.69E+00	1.71E+00	1.73E+00	2.08E+00
439.5	1.95E+00	1.97E+00	1.99E+00	2.39E+00

440.5	1.82E+00	1.84E+00	1.86E+00	2.23E+00
441.5	2.06E+00	2.09E+00	2.11E+00	2.53E+00
442.5	2.12E+00	2.14E+00	2.17E+00	2.60E+00
443.5	2.06E+00	2.08E+00	2.10E+00	2.52E+00
444.5	2.11E+00	2.13E+00	2.15E+00	2.58E+00
445.5	1.94E+00	1.96E+00	1.98E+00	2.38E+00
446.5	2.00E+00	2.02E+00	2.04E+00	2.45E+00
447.5	2.20E+00	2.23E+00	2.25E+00	2.70E+00
448.5	2.10E+00	2.12E+00	2.14E+00	2.57E+00
449.5	2.17E+00	2.19E+00	2.21E+00	2.65E+00

———

GLOBAL ATMOSPHERE WATCH REPORT SERIES

1. Final Report of the Expert Meeting on the Operation of Integrated Monitoring Programmes, Geneva, 2 -5 September 1980.

2. Report of the Third Session of the GESAMP Working Group on the Interchange of Pollutants Between the Atmosphere and the Oceans (INTERPOLL-III), Miami, USA, 27-31 October 1980.

3. Report of the Expert Meeting on the Assessment of the Meteorological Aspects of the First Phase of EMEP, Shinfield Park, U.K., 30 March - 2 April 1981.

4. Summary Report on the Status of the WMO Background Air Pollution Monitoring Network as at April 1981.

5. Report of the WMO/UNEP/ICSU Meeting on Instruments, Standardization and Measurements Techniques for Atmospheric CO_2, Geneva, 8-11; September 1981.

6. Report of the Meeting of Experts on BAPMoN Station Operation, Geneva, 23–26 November 1981.

7. Fourth Analysis on Reference Precipitation Samples by the Participating World Meteorological Organization Laboratories by Robert L. Lampe and John C. Puzak, December 1981.

8. Review of the Chemical Composition of Precipitation as Measured by the WMO BAPMoN by Prof. Dr. Hans-Walter Georgii, February 1982.

9. An Assessment of BAPMoN Data Currently Available on the Concentration of CO_2 in the Atmosphere by M.R. Manning, February 1982.

10. Report of the Meeting of Experts on Meteorological Aspects of Long-range Transport of Pollutants, Toronto, Canada, 30 November - 4 December 1981.

11. Summary Report on the Status of the WMO Background Air Pollution Monitoring Network as at May 1982.

12. Report on the Mount Kenya Baseline Station Feasibility Study edited by Dr. Russell C. Schnell.

13. Report of the Executive Committee Panel of Experts on Environmental Pollution, Fourth Session, Geneva, 27 September - 1 October 1982.

14. Effects of Sulphur Compounds and Other Pollutants on Visibility by Dr. R.F. Pueschel, April 1983.

15. Provisional Daily Atmospheric Carbon Dioxide Concentrations as Measured at BAPMoN Sites for the Year 1981, May 1983.

16. Report of the Expert Meeting on Quality Assurance in BAPMoN, Research Triangle Park, North Carolina, USA, 17-21 January 1983.

17. General Consideration and Examples of Data Evaluation and Quality Assurance Procedures Applicable to BAPMoN Precipitation Chemistry Observations by Dr. Charles Hakkarinen, July 1983.

18. Summary Report on the Status of the WMO Background Air Pollution Monitoring Network as at May 1983.

19. Forecasting of Air Pollution with Emphasis on Research in the USSR by M.E. Berlyand, August 1983.

20. Extended Abstracts of Papers to be Presented at the WMO Technical Conference on Observation and Measurement of Atmospheric Contaminants (TECOMAC), Vienna, 17-21 October 1983.

21. Fifth Analysis on Reference Precipitation Samples by the Participating World Meteorological Organization Laboratories by Robert L. Lampe and William J. Mitchell, November 1983.

22. Report of the Fifth Session of the WMO Executive Council Panel of Experts on Environmental Pollution, Garmisch-Partenkirchen, Federal Republic of Germany, 30 April - 4 May 1984 (WMO TD No. 10).

23. Provisional Daily Atmospheric Carbon Dioxide Concentrations as Measured at BAPMoN Sites for the Year 1982. November 1984 (WMO TD No. 12).

24. Final Report of the Expert Meeting on the Assessment of the Meteorological Aspects of the Second Phase of EMEP, Friedrichshafen, Federal Republic of Germany, 7-10 December 1983. October 1984 (WMO TD No. 11).

25. Summary Report on the Status of the WMO Background Air Pollution Monitoring Network as at May 1984. November 1984 (WMO TD No. 13).

26. Sulphur and Nitrogen in Precipitation: An Attempt to Use BAPMoN and Other Data to Show Regional and Global Distribution by Dr. C.C. Wallén. April 1986 (WMO TD No. 103).

27. Report on a Study of the Transport of Sahelian Particulate Matter Using Sunphotometer Observations by Dr. Guillaume A. d'Almeida. July 1985 (WMO TD No. 45).

28. Report of the Meeting of Experts on the Eastern Atlantic and Mediterranean Transport Experiment ("EAMTEX"), Madrid and Salamanca, Spain, 6-8 November 1984.

29. Recommendations on Sunphotometer Measurements in BAPMoN Based on the Experience of a Dust Transport Study in Africa by Dr. Guillaume A. d'Almeida. September 1985 (WMO TD No. 67).

30. Report of the Ad-hoc Consultation on Quality Assurance Procedures for Inclusion in the BAPMoN Manual, Geneva, 29-31 May 1985.

31. Implications of Visibility Reduction by Man-Made Aerosols (Annex to No. 14) by R.M. Hoff and L.A. Barrie. October 1985 (WMO TD No. 59).

32. Manual for BAPMoN Station Operators by E. Meszaros and D.M. Whelpdale. October 1985 (WMO TD No. 66).

33. Man and the Composition of the Atmosphere: BAPMoN - An international programme of national needs, responsibility and benefits by R.F. Pueschel, 1986.

34. Practical Guide for Estimating Atmospheric Pollution Potential by Dr. L.E. Niemeyer. August 1986 (WMO TD No. 134).

35. Provisional Daily Atmospheric CO_2 Concentrations as Measured at BAPMoN Sites for the Year 1983. December 1985 (WMO TD No. 77).

36. Global Atmospheric Background Monitoring for Selected Environmental Parameters. BAPMoN Data for 1984. Volume I: Atmospheric Aerosol Optical Depth. October 1985 (WMO TD No. 96).

37. Air-Sea Interchange of Pollutants by R.A. Duce. September 1986 (WMO TD No. 126).

38. Summary Report on the Status of the WMO Background Air Pollution Monitoring Network as at 31 December 1985. September 1986 (WMO TD No. 136).

39. Report of the Third WMO Expert Meeting on Atmospheric Carbon Dioxide Measurement Techniques, Lake Arrowhead, California, USA, 4-8 November 1985. October 1986.

40. Report of the Fourth Session of the CAS Working Group on Atmospheric Chemistry and Air Pollution, Helsinki, Finland, 18-22 November 1985. January 1987.

41. Global Atmospheric Background Monitoring for Selected Environmental Parameters. BAPMoN Data for 1982, Volume II: Precipitation chemistry, continuous atmospheric carbon dioxide and suspended particulate matter. June 1986 (WMO TD No. 116).

42. Scripps reference gas calibration system for carbon dioxide-in-air standards: revision of 1985 by C.D. Keeling, P.R. Guenther and D.J. Moss. September 1986 (WMO TD No. 125).

43. Recent progress in sunphotometry (determination of the aerosol optical depth). November 1986.

44. Report of the Sixth Session of the WMO Executive Council Panel of Experts on Environmental Pollution, Geneva, 5-9 May 1986. March 1987.

45. Proceedings of the International Symposium on Integrated Global Monitoring of the State of the Biosphere (Volumes I-IV), Tashkent, USSR, 14-19 October 1985. December 1986 (WMO TD No. 151).

46.   Provisional Daily Atmospheric Carbon Dioxide Concentrations as Measured at BAPMoN Sites for the Year 1984. December 1986 (WMO TD No. 158).

47.   Procedures and Methods for Integrated Global Background Monitoring of Environmental Pollution by F.Ya. Rovinsky, USSR and G.B. Wiersma, USA. August 1987 (WMO TD No. 178).

48.   Meeting on the Assessment of the Meteorological Aspects of the Third Phase of EMEP IIASA, Laxenburg, Austria, 30 March - 2 April 1987. February 1988.

49.   Proceedings of the WMO Conference on Air Pollution Modelling and its Application (Volumes I-III), Leningrad, USSR, 19-24 May 1986. November 1987 (WMO TD No. 187).

50.   Provisional Daily Atmospheric Carbon Dioxide Concentrations as Measured at BAPMoN Sites for the Year 1985. December 1987 (WMO TD No. 198).

51.   Report of the NBS/WMO Expert Meeting on Atmospheric CO_2 Measurement Techniques, Gaithersburg, USA, 15-17 June 1987. December 1987.

52.   Global Atmospheric Background Monitoring for Selected Environmental Parameters. BAPMoN Data for 1985. Volume I: Atmospheric Aerosol Optical Depth. September 1987.

53.   WMO Meeting of Experts on Strategy for the Monitoring of Suspended Particulate Matter in BAPMoN - Reports and papers presented at the meeting, Xiamen, China, 13-17 October 1986. October 1988.

54.   Global Atmospheric Background Monitoring for Selected Environmental Parameters. BAPMoN Data for 1983, Volume II: Precipitation chemistry, continuous atmospheric carbon dioxide and suspended particulate matter (WMO TD No. 283).

55.   Summary Report on the Status of the WMO Background Air Pollution Monitoring Network as at 31 December 1987 (WMO TD No. 284).

56.   Report of the First Session of the Executive Council Panel of Experts/CAS Working Group on Environmental Pollution and Atmospheric Chemistry, Hilo, Hawaii, 27-31 March 1988. June 1988.

57.   Global Atmospheric Background Monitoring for Selected Environmental Parameters. BAPMoN Data for 1986, Volume I: Atmospheric Aerosol Optical Depth. July 1988.

58.   Provisional Daily Atmospheric Carbon Dioxide Concentrations as measured at BAPMoN sites for the years 1986 and 1987 (WMO TD No. 306).

59.   Extended Abstracts of Papers Presented at the Third International Conference on Analysis and Evaluation of Atmospheric CO_2 Data - Present and Past, Hinterzarten, Federal Republic of Germany, 16-20 October 1989 (WMO TD No. 340).

60.   Global Atmospheric Background Monitoring for Selected Environmental Parameters. BAPMoN Data for 1984 and 1985, Volume II: Precipitation chemistry, continuous atmospheric carbon dioxide and suspended particulate matter.

61.   Global Atmospheric Background Monitoring for Selected Environmental Parameters. BAPMoN Data for 1987 and 1988, Volume I: Atmospheric Aerosol Optical Depth.

62.   Provisional Daily Atmospheric Carbon Dioxide Concentrations as measured at BAPMoN sites for the year 1988 (WMO TD No. 355).

63.   Report of the Informal Session of the Executive Council Panel of Experts/CAS Working Group on Environmental Pollution and Atmospheric Chemistry, Sofia, Bulgaria, 26 and 28 October 1989.

64.   Report of the consultation to consider desirable locations and observational practices for BAPMoN stations of global importance, Bermuda Research Station, 27-30 November 1989.

65.   Report of the Meeting on the Assessment of the Meteorological Aspects of the Fourth Phase of EMEP, Sofia, Bulgaria, 27 and 31 October 1989.

66.   Summary Report on the Status of the WMO Global Atmosphere Watch Stations as at 31 December 1990 (WMO TD No. 419).

67. Report of the Meeting of Experts on Modelling of Continental, Hemispheric and Global Range Transport, Transformation and Exchange Processes, Geneva, 5-7 November 1990.

68. Global Atmospheric Background Monitoring for Selected Environmental Parameters. BAPMoN Data For 1989, Volume I: Atmospheric Aerosol Optical Depth.

69. Provisional Daily Atmospheric Carbon Dioxide Concentrations as measured at Global Atmosphere Watch (GAW)-BAPMoN sites for the year 1989 (WMO TD No. 400).

70. Report of the Second Session of EC Panel of Experts/CAS Working Group on Environmental Pollution and Atmospheric Chemistry, Santiago, Chile, 9-15 January 1991 (WMO TD No. 633).

71. Report of the Consultation of Experts to Consider Desirable Observational Practices and Distribution of GAW Regional Stations, Halkidiki, Greece, 9-13 April 1991 (WMO TD No. 433).

72. Integrated Background Monitoring of Environmental Pollution in Mid-Latitude Eurasia by Yu.A. Izrael and F.Ya. Rovinsky, USSR (WMO TD No. 434).

73. Report of the Experts Meeting on Global Aerosol Data System (GADS), Hampton, Virginia, 11 to 12 September 1990 (WMO TD No. 438).

74. Report of the Experts Meeting on Aerosol Physics and Chemistry, Hampton, Virginia, 30 to 31 May 1991 (WMO TD No. 439).

75. Provisional Daily Atmospheric Carbon Dioxide Concentrations as measured at Global Atmosphere Watch (GAW)-BAPMoN sites for the year 1990 (WMO TD No. 447).

76. The International Global Aerosol Programme (IGAP) Plan: Overview (WMO TD No. 445).

77. Report of the WMO Meeting of Experts on Carbon Dioxide Concentration and Isotopic Measurement Techniques, Lake Arrowhead, California, 14-19 October 1990.

78. Global Atmospheric Background Monitoring for Selected Environmental Parameters BAPMoN Data for 1990, Volume I: Atmospheric Aerosol Optical Depth (WMO TD No. 446).

79. Report of the Meeting of Experts to Consider the Aerosol Component of GAW, Boulder, 16 to 19 December 1991 (WMO TD No. 485).

80. Report of the WMO Meeting of Experts on the Quality Assurance Plan for the GAW, Garmisch-Partenkirchen, Germany, 26-30 March 1992 (WMO TD No. 513).

81. Report of the Second Meeting of Experts to Assess the Response to and Atmospheric Effects of the Kuwait Oil Fires, Geneva, Switzerland, 25-29 May 1992 (WMO TD No. 512).

82. Global Atmospheric Background Monitoring for Selected Environmental Parameters BAPMoN Data for 1991, Volume I: Atmospheric Aerosol Optical Depth (WMO TD No. 518).

83. Report on the Global Precipitation Chemistry Programme of BAPMoN (WMO TD No. 526).

84. Provisional Daily Atmospheric Carbon Dioxide Concentrations as measured at GAW-BAPMoN sites for the year 1991 (WMO TD No. 543).

85. Chemical Analysis of Precipitation for GAW: Laboratory Analytical Methods and Sample Collection Standards by Dr Jaroslav Santroch (WMO TD No. 550).

86. The Global Atmosphere Watch Guide, 1993 (WMO TD No. 553).

87. Report of the Third Session of EC Panel/CAS Working Group on Environmental Pollution and Atmospheric Chemistry, Geneva, 8-11 March 1993 (WMO TD No. 555).

88. Report of the Seventh WMO Meeting of Experts on Carbon Dioxide Concentration and Isotopic Measurement Techniques, Rome, Italy, 7-10 September 1993, (edited by Graeme I. Pearman and James T. Peterson) (WMO TD No. 669).

89. 4th International Conference on CO_2 (Carqueiranne, France, 13-17 September 1993) (WMO TD No. 561).

90.   Global Atmospheric Background Monitoring for Selected Environmental Parameters GAW Data for 1992, Volume I: Atmospheric Aerosol Optical Depth (WMO TD No. 562).

91.   Extended Abstracts of Papers Presented at the WMO Region VI Conference on the Measurement and Modelling of Atmospheric Composition Changes Including Pollution Transport, Sofia, 4 to 8 October 1993 (WMO TD No. 563).

92.   Report of the Second WMO Meeting of Experts on the Quality Assurance/Science Activity Centres of the Global Atmosphere Watch, Garmisch-Partenkirchen, 7-11 December 1992 (WMO TD No. 580).

93.   Report of the Third WMO Meeting of Experts on the Quality Assurance/Science Activity Centres of the Global Atmosphere Watch, Garmisch-Partenkirchen, 5-9 July 1993 (WMO TD No. 581).

94.   Report on the Measurements of Atmospheric Turbidity in BAPMoN (WMO TD No. 603).

95.   Report of the WMO Meeting of Experts on UV-B Measurements, Data Quality and Standardization of UV Indices, Les Diablerets, Switzerland, 25-28 July 1994 (WMO TD No. 625).

96.   Global Atmospheric Background Monitoring for Selected Environmental Parameters WMO GAW Data for 1993, Volume I: Atmospheric Aerosol Optical Depth.

97.   Quality Assurance Project Plan (QAPjP) for Continuous Ground Based Ozone Measurements (WMO TD No. 634).

98.   Report of the WMO Meeting of Experts on Global Carbon Monoxide Measurements, Boulder, USA, 7-11 February 1994 (WMO TD No. 645).

99.   Status of the WMO Global Atmosphere Watch Programme as at 31 December 1993 (WMO TD No. 636).

100.   Report of the Workshop on UV-B for the Americas, Buenos Aires, Argentina, 22-26 August 1994.

101.   Report of the WMO Workshop on the Measurement of Atmospheric Optical Depth and Turbidity, Silver Spring, USA, 6-10 December 1993, (edited by Bruce Hicks) (WMO TD No. 659).

102.   Report of the Workshop on Precipitation Chemistry Laboratory Techniques, Hradec Kralove, Czech Republic, 17-21 October 1994 (WMO TD No. 658).

103.   Report of the Meeting of Experts on the WMO World Data Centres, Toronto, Canada, 17 - 18 February 1995, (prepared by Edward Hare) (WMO TD No. 679).

104.   Report of the Fourth WMO Meeting of Experts on the Quality Assurance/Science Activity Centres (QA/SACs) of the Global Atmosphere Watch, jointly held with the First Meeting of the Coordinating Committees of IGAC-GLONET and IGAC-ACE, Garmisch-Partenkirchen, Germany, 13 to 17 March 1995 (WMO TD No. 689).

105.   Report of the Fourth Session of the EC Panel of Experts/CAS Working Group on Environmental Pollution and Atmospheric Chemistry (Garmisch, Germany, 6-11 March 1995) (WMO TD No. 718).

106.   Report of the Global Acid Deposition Assessment (edited by D.M. Whelpdale and M-S. Kaiser) (WMO TD No. 777).

107.   Extended Abstracts of Papers Presented at the WMO-IGAC Conference on the Measurement and Assessment of Atmospheric Composition Change (Beijing, China, 9-14 October 1995) (WMO TD No. 710).

108.   Report of the Tenth WMO International Comparison of Dobson Spectrophotometers (Arosa, Switzerland, 24 July - 4 August 1995).

109.   Report of an Expert Consultation on 85Kr and 222Rn: Measurements, Effects and Applications (Freiburg, Germany, 28-31 March 1995) (WMO TD No. 733).

110.   Report of the WMO-NOAA Expert Meeting on GAW Data Acquisition and Archiving (Asheville, NC, USA, 4-8 November 1995) (WMO TD No. 755).

111.   Report of the WMO-BMBF Workshop on VOC Establishment of a "World Calibration/Instrument Intercomparison Facility for VOC" to Serve the WMO Global Atmosphere Watch (GAW) Programme (Garmisch-Partenkirchen, Germany, 17-21 December 1995) (WMO TD No. 756).

112. Report of the WMO/STUK Intercomparison of Erythemally-Weighted Solar UV Radiometers, Spring/Summer 1995, Helsinki, Finland (WMO TD No. 781).

112A. Report of the WMO/STUK '95 Intercomparison of broadband UV radiometers: a small-scale follow-up study in 1999, Helsinki, 2001, Addendum to GAW Report No. 112.

113. The Strategic Plan of the Global Atmosphere Watch (GAW) (WMO TD No. 802).

114. Report of the Fifth WMO Meeting of Experts on the Quality Assurance/Science Activity Centres (QA/SACs) of the Global Atmosphere Watch, jointly held with the Second Meeting of the Coordinating Committees of IGAC-GLONET and IGAC-ACE[Ed], Garmisch-Partenkirchen, Germany, 15-19 July 1996 (WMO TD No. 787).

115. Report of the Meeting of Experts on Atmospheric Urban Pollution and the Role of NMSs (Geneva, 7-11 October 1996) (WMO TD No. 801).

116. Expert Meeting on Chemistry of Aerosols, Clouds and Atmospheric Precipitation in the Former USSR (Saint Petersburg, Russian Federation, 13-15 November 1995).

117. Report and Proceedings of the Workshop on the Assessment of EMEP Activities Concerning Heavy Metals and Persistent Organic Pollutants and their Further Development (Moscow, Russian Federation, 24-26 September 1996) (Volumes I and II) (WMO TD No. 806).

118. Report of the International Workshops on Ozone Observation in Asia and the Pacific Region (IWOAP, IWOAP-II), (IWOAP, 27 February-26 March 1996 and IWOAP-II, 20 August-18 September 1996) (WMO TD No. 827).

119. Report on BoM/NOAA/WMO International Comparison of the Dobson Spectrophotometers (Perth Airport, Perth, Australia, 3-14 February 1997), (prepared by Robert Evans and James Easson) (WMO TD No. 828).

120. WMO-UMAP Workshop on Broad-Band UV Radiometers (Garmisch-Partenkirchen, Germany, 22 to 23 April 1996) (WMO TD No. 894).

121. Report of the Eighth WMO Meeting of Experts on Carbon Dioxide Concentration and Isotopic Measurement Techniques (prepared by Thomas Conway) (Boulder, CO, 6-11 July 1995) (WMO TD No. 821).

122. Report of Passive Samplers for Atmospheric Chemistry Measurements and their Role in GAW (prepared by Greg Carmichael) (WMO TD No. 829).

123. Report of WMO Meeting of Experts on GAW Regional Network in RA VI, Budapest, Hungary, 5 to 9 May 1997.

124. Fifth Session of the EC Panel of Experts/CAS Working Group on Environmental Pollution and Atmospheric Chemistry, (Geneva, Switzerland, 7-10 April 1997) (WMO TD No. 898).

125. Instruments to Measure Solar Ultraviolet Radiation, Part 1: Spectral Instruments (lead author G. Seckmeyer) (WMO TD No. 1066), 2001.

126. Guidelines for Site Quality Control of UV Monitoring (lead author A.R. Webb) (WMO TD No. 884), 1998.

127. Report of the WMO-WHO Meeting of Experts on Standardization of UV Indices and their Dissemination to the Public (Les Diablerets, Switzerland, 21-25 July 1997) (WMO TD No. 921).

128. The Fourth Biennial WMO Consultation on Brewer Ozone and UV Spectrophotometer Operation, Calibration and Data Reporting, (Rome, Italy, 22-25 September 1996) (WMO TD No. 918).

129. Guidelines for Atmospheric Trace Gas Data Management (Ken Masarie and Pieter Tans), 1998 (WMO TD No. 907).

130. Jülich Ozone Sonde Intercomparison Experiment (JOSIE, 5 February to 8 March 1996), (H.G.J. Smit and D. Kley) (WMO TD No. 926).

131. WMO Workshop on Regional Transboundary Smoke and Haze in Southeast Asia (Singapore, 2 to 5 June 1998) (Gregory R. Carmichael). Two volumes.

132.   Report of the Ninth WMO Meeting of Experts on Carbon Dioxide Concentration and Related Tracer Measurement Techniques (Edited by Roger Francey), (Aspendale, Vic., Australia).

133.   Workshop on Advanced Statistical Methods and their Application to Air Quality Data Sets (Helsinki, 14-18 September 1998) (WMO TD No. 956).

134.   Guide on Sampling and Analysis Techniques for Chemical Constituents and Physical Properties in Air and Precipitation as Applied at Stations of the Global Atmosphere Watch. Carbon Dioxide (WMO TD No. 980).

135.   Sixth Session of the EC Panel of Experts/CAS Working Group on Environmental Pollution and Atmospheric Chemistry (Zurich, Switzerland, 8-11 March 1999) (WMO TD No.1002).

136.   WMO/EMEP/UNEP Workshop on Modelling of Atmospheric Transport and Deposition of Persistent Organic Pollutants and Heavy Metals (Geneva, Switzerland, 16-19 November 1999) (Volumes I and II) (WMO TD No. 1008).

137.   Report and Proceedings of the WMO RA II/RA V GAW Workshop on Urban Environment (Beijing, China, 1-4 November 1999) (WMO-TD. 1014) (Prepared by Greg Carmichael).

138.   Reports on WMO International Comparisons of Dobson Spectrophotometers, Parts I – Arosa, Switzerland, 19-31 July 1999, Part II – Buenos Aires, Argentina (29 Nov. – 12 Dec. 1999 and Part III – Pretoria, South Africa (18 March – 10 April 2000) (WMO TD No. 1016).

139.   The Fifth Biennial WMO Consultation on Brewer Ozone and UV Spectrophotometer Operation, Calibration and Data Reporting (Halkidiki, Greece, September 1998)(WMO TD No. 1019).

140.   WMO/CEOS Report on a Strategy for Integrating Satellite and Ground-based Observations of Ozone (WMO TD No. 1046).

141.   Report of the LAP/COST/WMO Intercomparison of Erythemal Radiometers Thessaloniki, Greece, 13-23 September 1999) (WMO TD No. 1051).

142.   Strategy for the Implementation of the Global Atmosphere Watch Programme (2001-2007), A Contribution to the Implementation of the Long-Term Plan (WMO TD No.1077).

143.   Global Atmosphere Watch Measurements Guide (WMO TD No. 1073).

144.   Report of the Seventh Session of the EC Panel of Experts/CAS Working Group on Environmental Pollution and Atmospheric Chemistry and the GAW 2001 Workshop (Geneva, Switzerland, 2 to 5 April 2001) (WMO TD No. 1104).

145.   WMO GAW International Comparisons of Dobson Spectrophotometers at the Meteorological Observatory Hohenpeissenberg, Germany (21 May – 10 June 2000, MOHp2000-1), 23 July – 5 August 2000, MOHp2000-2), (10 – 23 June 2001, MOHp2001-1) and (8 to 21 July 2001, MOHp2001-2). Prepared by Ulf Köhler (WMO TD No. 1114).

146.   Quality Assurance in monitoring solar ultraviolet radiation: the state of the art. (WMO TD No. 1180), 2003.

147.   Workshop on GAW in RA VI (Europe), Riga, Latvia, 27-30 May 2002. (WMO TD No. 1206).

148.   Report of the Eleventh WMO/IAEA Meeting of Experts on Carbon Dioxide Concentration and Related Tracer Measurement Techniques (Tokyo, Japan, 25-28 September 2001) (WMO TD No 1138).

149.   Comparison of Total Ozone Measurements of Dobson and Brewer Spectrophotometers and Recommended Transfer Functions (prepared by J. Staehelin, J. Kerr, R. Evans and K. Vanicek) (WMO TD No. 1147).

150.   Updated Guidelines for Atmospheric Trace Gas Data Management (Prepared by Ken Maserie and Pieter Tans (WMO TD No. 1149).

151.   Report of the First CAS Working Group on Environmental Pollution and Atmospheric Chemistry (Geneva, Switzerland, 18-19 March 2003) (WMO TD No. 1181).

152.   Current Activities of the Global Atmosphere Watch Programme (as presented at the 14th World Meteorological Congress, May 2003). (WMO TD No. 1168).

153.   WMO/GAW Aerosol Measurement Procedures: Guidelines and Recommendations. (WMO TD No. 1178).

154. WMO/IMEP-15 Trace Elements in Water Laboratory Intercomparison. (WMO TD No. 1195).

155. 1st International Expert Meeting on Sources and Measurements of Natural Radionuclides Applied to Climate and Air Quality Studies (Gif sur Yvette, France, 3-5 June 2003) (WMO TD No. 1201).

156. Addendum for the Period 2005-2007 to the Strategy for the Implementation of the Global Atmosphere Watch Programme (2001-2007), GAW Report No. 142 (WMO TD No. 1209).

157. JOSIE-1998 Performance of EEC Ozone Sondes of SPC-6A and ENSCI-Z Type (Prepared by Herman G.J. Smit and Wolfgang Straeter) (WMO TD No. 1218).

158. JOSIE-2000 Jülich Ozone Sonde Intercomparison Experiment 2000. The 2000 WMO international intercomparison of operating procedures for ECC-ozone sondes at the environmental simulation facility at Jülich (Prepared by Herman G.J. Smit and Wolfgang Straeter) (WMO TD No. 1225).

159. IGOS-IGACO Report - September 2004 (WMO TD No. 1235), 68 pgs, September 2004.

160. Manual for the GAW Precipitation Chemistry Programme (Guidelines, Data Quality Objectives and Standard Operating Procedures) (WMO TD No. 1251), 186 pgs, November 2004.

161. 12th WMO/IAEA Meeting of Experts on Carbon Dioxide Concentration and Related Tracers Measurement Techniques (Toronto, Canada, 15-18 September 2003), 274 pgs, May 2005.

162. WMO/GAW Experts Workshop on a Global Surface-Based Network for Long Term Observations of Column Aerosol Optical Properties, Davos, Switzerland, 8-10 March 2004 (edited by U. Baltensperger, L. Barrie and C. Wehrli) (WMO TD No. 1287), 153 pgs, November 2005.

163. World Meteorological Organization Activities in Support of the Vienna Convention on Protection of the Ozone Layer (WMO No. 974), 4 pgs, September 2005.

164. Instruments to Measure Solar Ultraviolet Radiation: Part 2: Broadband Instruments Measuring Erythemally Weighted Solar Irradiance (WMO TD No. 1289), 55 pgs, July 2008, electronic version 2006.

165. Report of the CAS Working Group on Environmental Pollution and Atmospheric Chemistry and the GAW 2005 Workshop, 14-18 March 2005, Geneva, Switzerland (WMO TD No. 1302), 189 pgs, March 2005.

166. Joint WMO-GAW/ACCENT Workshop on The Global Tropospheric Carbon Monoxide Observations System, Quality Assurance and Applications (EMPA, Dübendorf, Switzerland, 24 – 26 October 2005) (edited by J. Klausen) (WMO TD No. 1335), 36 pgs, September 2006.

167. The German Contribution to the WMO Global Atmosphere Watch Programme upon the 225th Anniversary of GAW Hohenpeissenberg Observatory (edited by L.A. Barrie, W. Fricke and R. Schleyer (WMO TD No. 1336), 124 pgs, December 2006.

168. 13th WMO/IAEA Meeting of Experts on Carbon Dioxide Concentration and Related Tracers Measurement Techniques (Boulder, Colorado, USA, 19-22 September 2005) (edited by J.B. Miller) (WMO TD No. 1359), 40 pgs, December 2006.

169. Chemical Data Assimilation for the Observation of the Earth's Atmosphere – ACCENT/WMO Expert Workshop in support of IGACO (edited by L.A. Barrie, J.P. Burrows, P. Monks and P. Borrell) (WMO TD No. 1360), 196 pgs, December 2006.

170. WMO/GAW Expert Workshop on the Quality and Applications of European GAW Measurements (Tutzing, Germany, 2-5 November 2004) (WMO TD No. 1367).

171. A WMO/GAW Expert Workshop on Global Long-Term Measurements of Volatile Organic Compounds (VOCs) (Geneva, Switzerland, 30 January – 1 February 2006) (WMO TD No. 1373), 36 pgs, February 2007.

172. WMO Global Atmosphere Watch (GAW) Strategic Plan: 2008 – 2015 (WMO TD No. 1384), 108 pgs, August 2008.

173. Report of the CAS Joint Scientific Steering Committee on Environmental Pollution and Atmospheric Chemistry (Geneva, Switzerland, 11-12 April 2007) (WMO TD No.1410), 33 pgs, June 2008.

174. World Data Centre for Greenhouse Gases Data Submission and Dissemination Guide (WMO TD No. 1416), 50 pgs, January 2008.

175. The Ninth Biennial WMO Consultation on Brewer Ozone and UV Spectrophotometer Operation, Calibration and Data Reporting (Delft, Netherlands, 31-May – 3 June 2005) (WMO TD No. 1419), 69 pgs, March 2008.

176. The Tenth Biennial WMO Consultation on Brewer Ozone and UV Spectrophotometer Operation, Calibration and Data Reporting (Northwich, United Kingdom, 4-8 June 2007) (WMO TD No. 1420), 61 pgs, March 2008.

177. Joint Report of COST Action 728 and GURME – Overview of Existing Integrated (off-line and on-line) Mesoscale Meteorological and Chemical Transport Modelling in Europe (ISBN 978-1-905313-56-3) (WMO TD No. 1427), 106 pgs, May 2008.

178. Plan for the implementation of the GAW Aerosol Lidar Observation Network GALION, (Hamburg, Germany, 27 - 29 March 2007) (WMO TD No. 1443), 52 pgs, November 2008.

179. Intercomparison of Global UV Index from Multiband Radiometers: Harmonization of Global UVI and Spectral Irradiance (WMO TD No. 1454), 61 pgs, March 2009.

180. Towards a Better Knowledge of Umkehr Measurements: A Detailed Study of Data from Thirteen Dobson Intercomparisons (WMO TD No. 1456), 50 pgs, December 2008.

181. Joint Report of COST Action 728 and GURME – Overview of Tools and Methods for Meteorological and Air Pollution Mesoscale Model Evaluation and User Training (WMO TD No. 1457), 121 pgs, November 2008.

182. IGACO-Ozone and UV Radiation Implementation Plan (WMO TD No. 1465), 49 pgs, April 2009.

183. Operations Handbook – Ozone Observations with a Dobson Spectrophotometer (WMO TD No. 1469), 91 pgs, March 2009.

184. Technical Report of Global Analysis Method for Major Greenhouse Gases by the World Data Center for Greenhouse Gases (WMO TD No. 1473), 29 pgs, June 2009.

185. Guidelines for the Measurement of Methane and Nitrous Oxide and their Quality Assurance (WMO TD No. 1478), 49 pgs, September 2009.

186. 14th WMO/IAEA Meeting of Experts on Carbon Dioxide Concentration and Related Tracers Measurement Techniques (Helsinki, Finland, 10-13 September 2007) (WMO TD No. 1487), 31 pgs, April 2009.

187. Joint Report of COST Action 728 and GURME – Review of the Capabilities of Meteorological and Chemistry-Transport Models for Describing and Predicting Air Pollution Episodes (ISBN 978-1-905313-77-8) (WMO TD No. 1502), 69 pgs, December 2009, electronic version -July 2009.

188. Revision of the World Data Centre for Greenhouse Gases Data Submission and Dissemination Guide (WMO TD No.1507), 55 pgs, November 2009.

189. Report of the MACC/GAW Session on the Near-Real-Time Delivery of the GAW Observations of Reactive Gases, Garmisch-Partenkirchen, Germany, 6-8 October 2009 (WMO TD No. 1527)